

Fusion assays for model membranes: a critical review

Rafael B. Lira^{a,b,*} and Rumiana Dimova^{a,*}

^aMax Planck Institute of Colloids and Interfaces, Potsdam, Germany

^bMoleculaire Biofysica, Zernike Instituut, Rijksuniversiteit Groningen, Groningen, Netherlands

*Corresponding authors: E-mail: rafael.lira@rug.nl, Rumiana.Dimova@mpikg.mpg.de

Contents

1. Introduction	230
2. Membrane models	233
2.1 Submicron liposomes	233
2.2 Giant unilamellar vesicles	234
2.3 Supported lipid bilayers	235
3. Membrane fusogens	236
4. Detecting membrane fusion with reconstituted systems: working principle	237
5. Membrane fusion systems	241
5.1 Liposome ensemble assays	241
5.2 Single-vesicle fusion assays	244
5.2.1 <i>Single-vesicle fusion with a planar membrane</i>	245
5.2.2 <i>Single-vesicle fusion with immobilized vesicles</i>	249
5.2.3 <i>Other single-vesicle systems</i>	250
5.2.4 <i>Outlook: single-vesicle studies</i>	252
5.3 Giant vesicle fusion assays	252
5.3.1 <i>GUV-GUV fusion</i>	253
5.3.2 <i>Small vesicle-GUV fusion</i>	257
6. Conclusions	263
Acknowledgments	263
References	263

Abstract

Membrane fusion is a process used by cells in a number of seemingly unrelated processes. In cells, it is regulated by a set of fusion proteins present on the opposing fusing membranes and, depending on environmental cues and system specifics, membrane fusion can transit through certain fusion intermediates that are occasionally shared by different fusion events. Due to the high complexity and dynamics, membrane fusion is usually studied using reconstituted membrane models and fusion assays. Using these systems and a combination of fluorescent probes, it is possible to assign changes in fluorescence to the fusion reaction and to detect intermediates. Here, we critically

review the most commonly used membrane models and how they are used in resolving and quantifying fusion, comparing their main features and limitations. Depending on the model and assays, it is possible to quantify fusion efficiency under different conditions, extract mechanistic and kinetic parameters from fusion reactions, determine the role of accessory factors and the molecular parameters that regulate fusion.



1. Introduction

Cells execute a number of basic tasks that are necessary to their proper function necessary to life. They sense, signal and respond to external and internal cues while undergoing shape remodeling for adaptation to the milieu. One of the most striking and yet fundamental processes in cells, at the heart of cellular sensing and response, is membrane fusion. This process occurs for a variety of cellular compartments, such as internal organelles or the plasma membrane. Membrane fusion is essential to many activities, which may appear unrelated — the fusion of a sperm cells to an egg during fertilization, the release of hormones into the bloodstream or neurotransmitters in the synaptic cleft for neurotransmission, intracellular trafficking and signaling via endo/lysosome fusion and wound healing, or the infection of cells by enveloped viruses, to name a few [1–3]. The membranes involved in the fusion process undergo massive shape transformations aided by cellular components and fusion proteins located at the opposed, fusing membranes [4,5], but also by the specific lipid molecules [6]. Although the outcomes might seem rather distinct, these processes often share some of the molecular requirements and may appear to transit through similar pathways [7,8]. On the molecular level, simulations have shown that there are multiple pathways through which lipids rearrange in the course of fusion (e.g. splayed lipids acting as cross-linkers between the adjacent membranes, poration of a hemifused diaphragm, rim-pore expansion, stalk formation exhibited by a small, disordered membrane patch formed by the two bilayers) [9–13]. However, these pathways are difficult, if not impossible, to resolve experimentally and depending on the degree of sensitivity of the employed technique, may appear similar.

In order for membranes to fuse, they first must come into close contact (Fig. 1). This implies overcoming the electrostatic, hydration and steric effects between the opposing lipid bilayers. This is followed by local bilayer destabilization, a process that involves morphological deformations of the

membrane and formation of non-bilayer intermediates, see e.g. Fig. 1B,C for images obtained from molecular dynamic or coarse-grained simulations [9,14]. The outer leaflets of the opposing membranes can mix forming a lipid stalk, characterized by an hourglass morphology. The lipid stalk may expand forming a hemifusion diaphragm. At this stage, the membranes have hemifused, but the aqueous compartments are still separated by a single bilayer. The hemifusion intermediate is favored by lipids that prefer to form hexagonal phases such as phosphatidylethanolamine, and it has been experimentally shown that these lipids are enriched in the highly curved stalk [15]. Finally, an aqueous fusion pore is formed, a region in the bilayer that connects the aqueous compartments of the fusing bilayers and that is lined by the lipid headgroups. In multicomponent systems, this intermediate can be stabilized by lipids with positive spontaneous curvature. It is still debatable whether in cells this structure is lined only by lipids or whether proteins are also lining the pore [16,17], although the fusion pore can also be formed in lipid-only membranes [18]. The fusion pore allows the mixing of the inner leaflet lipids and the passage of certain hydrophilic molecules provided they are smaller than the pore diameter [19]. The pore may close, returning the membranes back to the stalk structure, or it may collapse, leading to the complete merging of the fusion membranes and their aqueous compartments, resulting in full fusion [20,21]. Upon complete fusion, both lipids and aqueous solutions are fully mixed, and the fused membranes contain the sum of the lipid areas and volumes of the otherwise separate membranes and compartments. In other words, fusion is accompanied by increase in compartment size in area and volume [22].

Not surprisingly, membrane fusion in cells is a very complex process, which requires an exquisite number of fusion drivers and regulatory proteins that control its dynamics and transition through the fusion intermediates. These players set the time, speed and location for fusion to occur. In different cells and under different circumstances, membrane fusion may be a rare or a frequent event and individual fusion events may be rather fast or relatively slow. In extreme cases such as in neurons, fusion can be completed in only a few milliseconds [23,24]. Therefore, due to the high complexity and dynamics, membrane fusion is often studied using reconstituted systems using *membrane fusion assays*. Here, the role of individual or a set of proteins, regulatory molecules or biophysical properties can be studied separately, in well controlled conditions and each aspect can be potentially manipulated with good spatial and temporal precision. These assays have been proven very valuable in revealing and defining the molecular

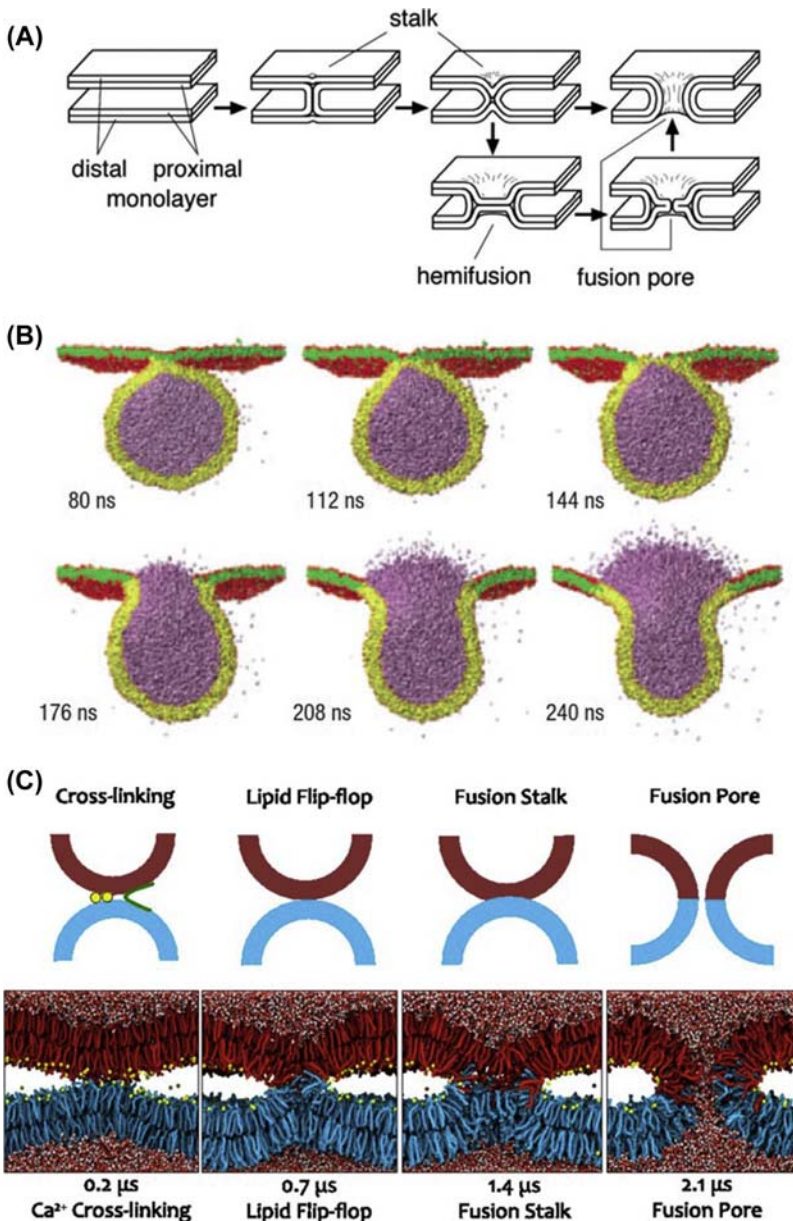


Fig.1 Transition states in membrane fusion and different ways of membrane representation with increasing degree of molecular detail (sheet-like, coarse-grained and all-atom). (A) Schematic presentation of the monolayers as smooth and bendable sheets as described by the stalk hypothesis. Reprinted from Ref. [2]. Copyright (2003), with permission from Elsevier. (B) Fusion event between a 28-nm-diameter vesicle and a tense bilayer obtained from coarse-grained simulations. Only particles representing

determinants as well as the physical properties that regulate and ultimately lead to fusion. Here, we review the most popular assays used to study membrane fusion. More specifically, we describe the main membrane models, the assays principles of operation, the methods of detection, the type of molecular, kinetic and physical information the specific assay is capable of producing, and their advantages and limitations. Combined, they permit the collection of mechanistic, kinetic, morphological and mechanical data down to the level of a single interacting fusion partner.



2. Membrane models

Many cellular processes can be studied using biomimetic models. With them, it is possible to reconstitute the necessary conditions of a given process but without the interference of cellular factors that are only indirectly involved. Not surprisingly, there are many membrane models designed for a variety of applications. Their close resemblance with biological membranes permits the study of membrane properties with the advantage of easy control over the system. These properties can be modulated by simply changing the composition of the membrane constituents and the medium where the membranes are dispersed. Here, we briefly review three of the most popular membrane models that are used on the study of membrane fusion, namely (i) submicroscopic small and large unilamellar vesicles, (ii) giant unilamellar vesicles and (iii) supported lipid bilayers. We briefly summarize the basic properties of each system and highlight their features and limitations when used as models for membrane fusion.

2.1 Submicron liposomes

The membrane model that was presumably described first consisted of lipid vesicles and vesicular aggregates reported decades ago by Bangham [25]. Due to their closed vesicular structure, they were later called *liposomes*. These



groups of water molecules (purple) initially located inside the vesicle are shown. The rare occurrence of a lipid spontaneously leaving the planar membrane and re-entering it is visible in the first two snapshots. Reprinted from Ref. [9] by permission from Springer Nature. Copyright (2005). (C) Top: Schematic drawing of vesicle fusion—lipid cross-linking, stalk initialization, and subsequent onset of stalk formation through lipid flip-flop. Bottom: Time evolution of the fusion of a two-bilayer system mediated by calcium (yellow dots) as obtained from all-atom molecular dynamics simulations. Reproduced from Ref. [14]. Copyright (2018) National Academy of Sciences.

vesicles feature a number of different structures, and their nomenclature refers to their size and complexity. Here, we focus on small and large unilamellar vesicles (SUVs and LUVs, respectively) – liposomes made of a single lipid bilayer with sizes of ~ 50 nm and ~ 100 nm, respectively. Due to their small size, their membranes are highly curved and they can exhibit substantial membrane tension, which is pronounced in SUVs rendering them less stable than LUVs. Vesicle size and structure can be easily controlled depending on the preparation [26]. They comprise a lipid bilayer with a hydrophobic core encapsulating an aqueous compartment, and therefore both hydrophobic and hydrophilic materials could be incorporated. Within this size range, SUVs and LUVs are smaller than the resolution of optical microscopy, and therefore they are not optically resolvable. For this reason, most experiments using SUVs and LUVs are performed using bulk, ensemble methods and spectroscopic techniques. More specifically, scattering methods are classically used to study vesicle structure and properties in general [27]. Nevertheless, it is possible to fluorescently label these vesicles using lipid analogs, or alternatively encapsulate water-soluble fluorescent molecules in the lumen, and study those using fluorescence-based techniques. More recently, super-resolution microscopy [28] and modern microscopic approaches have enabled the detection of single vesicles with fluorescence microscopy [29]. Membrane fusion assays rely on various combinations of scattering and fluorescence-based techniques to study fusion using SUVs and LUVs.

2.2 Giant unilamellar vesicles

Depending on the preparation method, it is possible to produce vesicles that are large enough to be observed under the microscope. These vesicles are called *giant unilamellar vesicles* (GUVs) when comprised of a single lipid bilayer. Morphologically, they are similar to SUVs and LUVs, but are much larger with sizes in the range of 10–100 μm . This enlarged size makes them especially useful models because it allows the direct observation and manipulation under the microscope [30–33], see also the detailed extended collection of studies in Ref. [34]. Their large size is similar to that of cells and they do not suffer from curvature effects associated with their smaller counterparts – GUV membranes are flat at the molecular level. These features make them very useful mimics of the plasma membrane. They can also encapsulate lipid and water-soluble molecules, permitting easy fluorescence microscopy experiments. GUVs are easily manipulated, and it is possible to move them from one region to another (i.e. to bring them in contact with a

target) using different micromanipulation techniques such as micropipettes, optical trapping, electric fields [34]. Finally, GUVs permit exchange of the external medium using microfluidic devices (i.e. to add or remove specific components [35]). When performed under the microscope, experiments with GUVs can be used to detect membrane responses such as budding, tubulation, and stability and localization of domains, features that are much more difficult (or often not even possible) with their smaller counterparts. Furthermore, the amount of lipids used in GUV experiments (typically sub-micromolar concentration) are orders of magnitude lower compared to bulk experiments with LUVs and SUV (millimolar concentrations).

2.3 Supported lipid bilayers

A rather different membrane model consists of flat bilayer patches formed on a solid surface, termed *supported lipid bilayers* (SLBs). Their flat topology makes them especially suitable with surface-sensitive techniques such as total internal reflection microscopy (TIRF). Using TIRF, it is possible to achieve high spatial resolution since excitation is confined to surface, especially important when compared to relatively slow confocal microscopy imaging. Therefore, SLBs are usually the model of choice for the detection of fast processes that occur on a surface. However, the strong interactions with the support imposes constraints to the membrane molecules (i.e. lipids), which are subject to high friction. As a result, molecules in SLBs have a largely reduced mobility or are even fully immobilized [36,37]. In general, the SLB and the solid support are separated by a thin layer of water, limiting the appropriate accommodation of large membrane proteins, which can potentially cause protein denaturation, or the incorporation of lipids as the membranes fuse. The strong interaction between the SLB and the support increases tension as well as sterically hinders the mobility of molecules embedded in it. Some approaches to increase the spacing and decrease interactions include the formation of the bilayer on a polymer functionalized surface that functions as a “cushion”, which is shown to recover molecular mobility to values similar to free-standing bilayers [38]. Another alternative includes the spreading of a large patch of membranes on spaced pillars. The membranes will be spread on areas that alternate between the pillar part and the gap part of the pillar substrates, thus forming supported and free-standing membranes regions [39]. This system is called pore-spanning membranes (PSMs). Whereas the supported areas display the features of SLBs, the behavior of lipid and protein molecules on the free-standing areas are

very similar to that on GUVs. Novel systems include the formation of GUVs where the whole membrane is supported by a fluid oil-water interface [40], and future applications with this system are still to be reported.

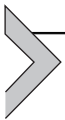


3. Membrane fusogens

As previously mentioned, the fusion of two bilayer membranes requires that these membranes come into close proximity in order to destabilize their bilayer structure. The kinetic rates at which these processes occur are governed by free energy barriers that reflect the underlying molecular (re)arrangements. Fusion of lipid bilayers is strongly suppressed by high barriers arising from effectively repulsive molecular forces. In cells, these energy barriers are reduced locally by specialized proteins, thereby strongly increasing the fusion rate in well-defined locations. The density of these localized fusion events must be sufficiently low to preserve the overall stability of the different membrane compartments. Indeed, if the free energy barriers for fusion were reduced in a global manner, all cellular membranes would merge and the cells would eventually collapse into a large membrane blob, also fusing with other cells, a situation clearly incompatible with life. Therefore, there must exist a *trigger*, or a fusogenic cue that brings opposing membranes in contact for fusion. Anything that triggers fusion of lipid bilayers is called a *fusogen*, and nature has created a few of them. In biology, fusion is mediated by a complementary set of proteins located in the opposing membranes destined to fusion. In cells, the most popular fusogenic molecules are a protein family termed SNAREs (soluble N-ethylmaleimide sensitive fusion attachment protein receptors) [41]. Other substances not present in cells can also be fusogenic, such as the fusion proteins present on the surface of enveloped viruses [3], or synthetic molecules.

There are a number of cues that drive membrane fusion. They include certain cell-penetrating peptides [14], some polymers [42], ions [43], and physical stimuli such as electric field [44]. In general, the fusogens induce membrane fusion by similar pathways transiting through the same intermediate steps found in cells, although they might largely differ in dynamics. Polymers and ions decrease the energy barrier for fusion by reducing the hydration layer between the opposing membranes [42]. Ions with strong membrane affinity confer electrostatic charge to the membranes that favors interaction, but they also increase tension through membrane condensing effects [45], which is known to facilitate fusion [9,46]. Similarly, membranes

can be rendered charged by the inclusion of charged lipids, whereby fusion is promoted by electrostatic interactions [47]. One of the few exceptions to the pathways of fusion is electroporation. When membranes in contact are electroporated and the pores on the opposing membranes are formed in the same area, the membranes fuse directly, “skipping” the other fusion intermediates. Therefore, there are different ways of fusing membranes, and different membrane models that could be used to study membrane fusion. In general, any fusogen could be used with any membrane model with few exceptions, and the choice of the fusogen and the model system will depend on the degree of complexity and the questions to be answered.



4. Detecting membrane fusion with reconstituted systems: working principle

Having introduced the main features of the most popular membrane fusion systems, we now describe how these systems are used as assays to study membrane fusion. Although these assays often vary substantially in their details, they mostly combine the following two features: (i) the use of synthetic or natural lipid vesicles as one (or both) of the fusion components, and (ii) detection of fusion using fluorescence or scattering signal as a readout. The lipid vesicles fuse with other vesicles or with planar bilayers. Depending on the topology and size of the fusing membranes, they are typically meant to mimic intracellular vesicles fusing with other vesicles or with the plasma membrane. In their simplest form, the membranes contain only lipids. More complex membranes contain additional components, or are derived from biological membranes.

Most fusion assays rely on fluorescence as a reporter of membrane fusion. For some dyes, one employs the effect that at high concentration the dyes exhibit (self-)quenching as a result of reabsorption processes from a neighboring dye molecule. This process is reversible, and dye dilution results in increase in fluorescence. For vesicles containing self-quenching concentrations of dyes, fusion leads to reduction of quenching and the fluorescence increases as the molecules redistribute into the new membranes or get diluted in the new aqueous compartment. This is valid for both lipid analogs present in the membrane or water-soluble dyes encapsulated in the aqueous compartments of vesicles, which will report lipid mixing and content mixing, respectively. Typically, self-quenching concentration of dye analogs in the membrane is above ~ 5 mol% of total lipid, whereas the concentration of encapsulated water-soluble dyes is higher than ~ 50 mM. Conversely, the

experiments can be performed in the presence of a fluorescence quencher. Depending on the location of the dye and the quencher, fusion will result in fluorescence increase or decrease. Consider a situation where one liposomal population contains the dye, whereas the other population contains the quencher. In that case, fusion will result in fluorescence quenching and a reduction in intensity. On the other hand, if both the dye and the quencher are present in one liposomal population and the second population contains a molecule that chelates the quencher, fusion will result in an increase in fluorescence because the quencher will be sequestered, thus relieving the dye fluorescence. Usually, experiments with fluorescence quenchers are performed using dye concentrations below self-quenching regimes. *Fluorescence resonance energy transfer* (FRET) represents a variant of this method, in which the quencher is a fluorescent dye itself. Depending on the localization of the donor and the acceptor FRET molecules, fusion can result in increase or decrease in donor or acceptor fluorescence after fusion. The magnitude and speed of changes in fluorescence are used to obtain mechanistic and kinetics information. It is important to mention that quenching is a non-linear process, and this should be taken into account when used to obtain quantitative data from fusion processes. It is also possible to perform the experiments using lower (non-quenching) dye concentrations. In this case, fusion does not result in an increase in fluorescence, but simply to the transfer of the dye to the non-labeled membrane population (the signal in this case, might be low and comparable to noise levels). Fluorescence can also be detected by other fluorescent methods, such as anisotropy, and fluorescence lifetime. The principle consists in detecting the associated changes of the respective parameter upon membrane fusion. For example, in the self-quenching regime or in the presence of a quencher, fluorescence lifetime is shortened. After fusion, dilution will result in longer fluorescence lifetime of the donor and this can similarly be used as an indication of fusion.

Depending on how fluorescence changes, it is possible to detect a number of fusion intermediates. Mixing membranes in fusogenic conditions and detecting the changes in the fluorescence signal (i.e. intensity, lifetime, FRET, anisotropy) can be performed spectroscopically in a cuvette or directly under the microscope. Consider a situation where one of the fusing membranes contains both lipid and content markers both at self-quenching concentrations. When the membranes are in contact and the contact zone is small, membrane docking will be difficult to detect as there is no molecular exchange, and thus no dye dilution (Fig. 2A). Hence, if the assay relies simply on fluorescence changes, such as those based on spectroscopic methods,

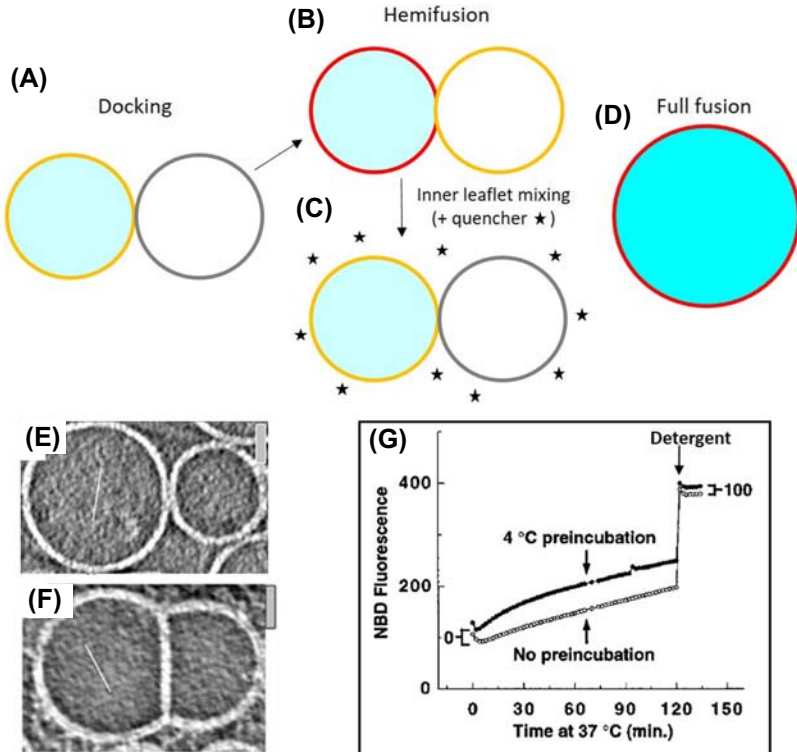


Fig.2 Detection of membrane fusion intermediates. (A) Sketch of two docked vesicles, one of which encapsulates water-soluble dye (light blue) and its membrane is labeled with a fluorescent dye (yellow), whereby both dyes are at self-quenching concentrations. (B) Hemifusion results in dequenching of the membrane dye leading to a stronger signal from the originally labeled vesicle (red) and the transfer of membrane dye to the non-labeled vesicle (yellow). (C) If then a fluorescence quencher is added externally (stars), only the lipids in the outer leaflet are quenched. (D) Full fusion results in a larger vesicle with brighter membrane (red) and brighter interior (blue). (E, F) Vesicle docking and hemifusion as observed by electron microscopy; scale bars correspond to 25 nm. Reproduced with permission from Ref. [133]. (G) Typical fluorescence signal changes associated with membrane fusion, see text for detail. Adapted from Ref. [52]. Copyright (1998), with permission from Elsevier.

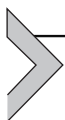
docking will not be detectable. It is, nevertheless, possible to detect docking using microscopy. If both populations are labeled with a FRET pair, docking will result in co-localized fluorescence without changes in FRET [48]. Alternatively, docking can be detected by electron microscopy, in which case the contact area will contain a double bilayer (Fig. 2E) [49]. It is also possible to detect docking more indirectly using dynamic light scattering

of LUV suspensions. Interacting vesicles will form larger aggregates than single vesicles. If two vesicles dock, their size will be the sum of the diameters of the individual vesicles plus the hydration layer [50]. Note that the last two methods do not require fluorescence labeling. As an alternative, confocal microscopy observation of GUV suspension would provide a direct evidence for docking visualized by adhesion of vesicles in contact [51] whereby a relatively flat contact zone forms if the vesicles are deflated.

If hemifusion takes place, the outer leaflets of the fusing bilayers will mix, but the inner leaflets will not. This results in some degree of dequenching of the lipid dyes and an increase in membrane fluorescence (Fig. 2B). However, in LUV-based assays it is usually not possible to ascribe the small changes in fluorescence to hemifusion or to some degree of full fusion (or a combination of both) — note that much hemifusion and some degree of full fusion will both produce similar dequenching. For this reason, another approach is usually used to discriminate between hemifusion and full-fusion. The addition of a water-soluble and membrane impermeable fluorescent quencher to the vesicle suspension is used to check for inner leaflet mixing: only the fluorescent dyes present in the outer leaflet will be quenched [52]. Upon hemifusion, lipid dyes from the outer leaflet are diluted and fluorescence increases. After the addition of the quencher, hemifusion is detected as the fluorescence decreases to levels before fusion because all the dyes that contributed to the increase in fluorescence will be quenched (Fig. 2C). Conversely, if mixing of the inner leaflet lipids occurs as well, the addition of quencher will decrease fluorescence by \sim half, since inner leaflet lipids will be protected. Using electron microscopy, the interacting portion of the hemifused membrane will consist of a single bilayer, and the fusing vesicles will have an hour-glass shape (Fig. 2F). The assays can be applied for GUV-GUV hemifusion as well [51].

If a fusion pore opens but does not expand, the inner leaflets will mix but this would not necessarily mean that the membranes have fully merged. In that case, the interpretation from the inner leaflet mixing assay using a lipid quencher may be erroneous. The detection of full fusion is done by encapsulating a self-quenched water-soluble dye in one vesicle population and detecting dequenching by dilution — content mixing (Fig. 2D) [53]. Upon full fusion, both the lipid and the content signal must increase. However, care should be taken because vesicle rupture, which may be quite common depending on the experimental conditions, will also result in an increase in fluorescence due to leakage and could be erroneously interpreted as signal from full fusion. One way to circumvent this is by performing

content mixing in the presence of a fluorescent quencher in the outside medium, in which leakage will not produce an increase in fluorescence. Alternatively, detecting both lipid and content mixing might be more informative. And of course, observations on GUV samples can directly show whether vesicle rupture occurs.



5. Membrane fusion systems

Above, we have described how the changes in fluorescence of the dyes present in the membrane or encapsulated into the aqueous core report the fusion process. These concepts are general and applicable to membranes of any topology (vesicles, planar membranes, cells). Below, we describe the different fusion assays that use the concepts above to study membrane fusion. We classify the various fusion assays into (i) bulk/ensemble assays, (ii) single-vesicle assays and (iii) GUV-based assays, and summarize the type of information that can be obtained with each of them. We will often use the term “fusion efficiency”, which is a measure of the degree of membrane fusion in a specific assay, occasionally compared to a control where the signal is maximal. Because the definition of the term varies with the used assay and is not always well defined, it might only indirectly refer to fusion efficiency hindering cross-comparisons between the used assays.

5.1 Liposome ensemble assays

The year 1998 witnessed a hallmark in the field of membrane fusion, when Weber et al. demonstrated that only three proteins were sufficient to trigger membrane fusion. They were termed *the minimal machinery* responsible for membrane fusion [52]. Instead of using genetic manipulations of cells, they reconstituted complementary SNARE proteins into two populations of small liposomes. When mixed, SNARE-reconstituted liposomes were shown to fuse without the need of additional catalyst or other components, grounding the foundations of fusion systems based on reconstituted proteins. Although this is an outstanding example of the use of reconstituted assays to simulate *in vivo* processes, the fusion assay used by the researchers was in fact reported much earlier [54–57]. The assay employed FRET-based dequenching, where one liposomal population contained a FRET pair, namely lipid analogs conjugated with N-(7-nitro-2-1,3-benzoxadiazol-4-yl) (NBD) and rhodamine (Rh), as the donor and acceptor, respectively. Fig. 2G shows the time trace in a typical experiment. Upon fusion, the

dyes are diluted in the non-labeled liposomal population, dequenching NBD fluorescence. Similarly to the situation *in vivo*, at low temperature SNARE proteins do not promote fusion, and docked intermediates accumulate (although resolving docking is not feasible since there is no associated change in fluorescence). Raising the temperature results in SNARE-mediated membrane fusion, thus leading to an increase in donor fluorescence (Fig. 2G). Pre-incubation of SNARE vesicles at 4 °C improves the extent and speed of fusion compared to direct incubation at physiological temperature because docked intermediates accumulate, thus suggesting that docking, not fusion is rate limiting. At the end of the experiment, the vesicles are solubilized by detergents to obtain the maximum possible increase in NBD fluorescence.

Regardless of the location of the dye, whether in the membrane or encapsulated into the aqueous core, the increase in intensity is only partial, as the dilution from labeled to non-labeled vesicles is not infinite. Note in Fig. 2G that vesicle solubilization by detergent results in additional dequenching. In these experiments, the increase in fluorescence due to fusion is normalized to the maximum possible fluorescence after detergent solubilization. Although this can be very informative when comparing different fusion conditions, this approach measures fusion efficiency only indirectly, and the quantification of how much membrane (i.e. how many vesicles) has been involved in fusion cannot be obtained.

More specifically, the experiments discussed above show that SNARE proteins reconstituted in liposomes lead to membrane merging, however, with very slow dynamics compared to *in vivo* fusion, which is on the order of milliseconds. In addition, fusion in cells is controlled by regulatory proteins, such as the calcium sensor protein synaptotagmin (syt). Thus, two main aspects of fusion, namely fusion speed and control, were still to be demonstrated using reconstituted systems. Tucker et al. addressed the latter by co-reconstitution of syt in SNARE liposomes. Syt enhances both fusion extent and speed in the presence of calcium, whereas it suppresses fusion in the absence of the divalent ions [58]. Thus, syt alone functions as a calcium sensor that regulates membrane fusion. These results were specific to syt and calcium; disruption of the calcium-binding domains abolishes syt stimulation of fusion. In addition, syt-based increase in fusion depends on negatively-charged lipids; increasing the fraction of PS in the membrane enhances syt-mediated fusion.

Other liposomal ensemble experiments have clarified many of the roles of SNAREs and accessory fusion proteins on different processes associated

with membrane fusion. They include resolving the number of SNARE molecules required to drive fusion [59], how accessory proteins regulate SNARE-mediated fusion [60], and fusion intermediates [61], the role of lipid geometry on fusion [62,63], the demonstration that SNARE fusion involves leaky intermediates [64], to mention a few. Although these studies may differ in the type of process they address, they all have in common that fusion was assessed from lipid mixing. Lipid mixing is a required but it is not a sufficient indicator for full fusion and therefore, experiments with content mixing are required. Reports with content mixing are much rarer compared to lipid mixing. In one of them, Nickel et al. used complementary DNA oligonucleotides encapsulated inside two individual liposomal populations [65]. One of the DNAs was labeled with radioactive ^{33}P isotope and its complement was labeled with biotin. After fusion, SNARE-reconstituted liposomes were solubilized by detergents, DNA was immobilized on a streptavidin-coated surface and full fusion was assessed from radioactive signal. They found that SNAREs alone suffice for full fusion. Not surprisingly, given the use of radiation, this approach is not very popular. More frequently, content mixing is probed using dequenching of encapsulated water-soluble dyes. Using $\text{Tb}^{+3}/\text{DPA}$ as a dye/quencher reporter, Dennison et al. showed that SNAREs alone do not promote full fusion, in contrast to the findings as above [66]. Instead, full fusion was demonstrated only after addition of high concentrations of PEG. Apart from the deficiencies of the assays, these results suggest that in cells, full fusion likely requires additional proteins, since SNAREs alone do not promote full fusion or they do so very slowly. A more recent study addressed the issue above by encapsulating sulforhodamine in one liposomal population at self-quenching concentrations. SNARE-mediated fusion driving content mixing was observed by sulforhodamine dequenching, and this was promoted by the regulatory Munc18c protein [67]. Variations of these assays exist, and include the use of two content markers that form a FRET pair, where fusion is detected by the changes in FRET upon content mixing [62]. The use of additional dyes has permitted the detection of lipid and content mixing in the same experiment, which is very important because fusion intermediates could be simultaneously detected in the same fusing population. Using this approach, Liu et al. confirmed that SNARE-mediated membrane fusion is aided by accessory proteins [68].

Although ensemble assays have proven very useful to unravel many aspects of membrane fusion, they have significant limitations. First, self-quenching is not necessarily a linear process. Second, the degree of fusion

(usually defined as the degree of dequenching) is typically compared to the maximum possible dequenching signal upon vesicle solubilization by detergents whereby the probe can be diluted to different concentration levels; in other words, it is simply an indirect estimation that is sensitive to the experimental conditions (i.e. liposome or dye concentration). Third, the rate of fluorescence increase, used to determine fusion kinetics, often displays complex behavior, and thus the extraction of quantitative data is not always straightforward. Fourth, it is very difficult, if not impossible, to decouple the role of fusion intermediates on kinetics when trying to pinpoint for the rate-limiting steps. Fifth, as an ensemble assay, the data is convoluted over thousands to millions of fusion events, and the data obtained are average out over the whole population. As a result, individual short-lived or rare events are lost. Sixth, it is also difficult to achieve fast and controlled mixing of the fusing partners using populations of liposomes in a cuvette, usually performed manually, and detect the onset of (lipid or content) mixing before any fusion has occurred. Seventh, often leakage of the liposomes can occur, and because of contacts and/or changes in membrane tension can be interpreted as fusion signal. Lastly, the assay is insensitive to many fusion intermediates, requiring additional tests to check for the type of intermediate, such as a separate inner leaflet mixing test to distinguish lipid mixing only from content mixing. The development of new assays that are able to directly detect and resolve single fusion events came to circumvent these limitations. Advances in microscopy imaging, sample preparation and handling as well as imaging processing have enabled the detection of the fusion processes that occur on a single-vesicle level with millisecond time resolution.

5.2 Single-vesicle fusion assays

Advances in fluorescence microscopy enables direct observations of single vesicles. This brings several important advantages for studying membrane fusion when compared to ensemble assays. It is possible to directly observe the fusing species and their association with regulatory factors to detect individual behavior, and thus group species into distinct populations, which is especially important for heterogeneous systems. Furthermore, membrane intermediates can be directly resolved. The general principle of detecting the fusion of a single vesicle with another membrane consists of labeling lipid vesicles with fluorescent dyes and the detection of fusion using fluorescence microscopy. As with bulk assays, the vesicles can be labeled at their membrane or their aqueous interior (or both) to study lipid and content mixing,

respectively. In general, one of the fusing species (membrane) is immobilized, whereas the other one is free to diffuse, bind and fuse to the immobile target membrane. Two main approaches for single-vesicle fusion employ (i) vesicle fusion to a supported lipid bilayer or, (ii) vesicle fusion to vesicles immobilized on a surface. The majority of studies based on these approaches employ LUVs and SUVs. In the following subsections, we will refer to them simply as vesicles unless studies with giant vesicles are described. Synthetic as well as natural vesicles derived from cells can be used. Direct observation of fusion events in real time permits distinguishing fusion from other competing membrane processes such as vesicle aggregation and leakage, which are only indirectly assessed with ensemble assays.

5.2.1 Single-vesicle fusion with a planar membrane

Individual vesicles can fuse to a planar membrane, either supported on a surface or free-standing. The planar membrane is the “acceptor” for incoming fusion of “donor” vesicles and this configuration mimics the curvatures found in the fusion of intracellular vesicles with the plasma membrane. Often, the immobilized membrane is also labeled so as its position and fusion site can be precisely located. A quality control test is often employed to check membrane homogeneity and fluidity by photobleaching a small segment of the membrane. Fast and full recovery validates its quality [69]. The way membrane fluorescence changes relate to membrane fusion and its intermediates depending on the labeling scheme. The arrival and docking of the mobile fluorescent vesicle are seen as the appearance of a fluorescent, diffraction-limited spot (Fig. 3). If the fluorescence does not change with time, it means that the vesicle is simply docked at the membrane and does not proceed to fusion nor detaches. If the membrane and/or content is labeled at quenching conditions, fusion results in dye dequenching and a burst in fluorescence is observed (Fig. 3B). Afterward, the fluorescence signal decreases as the dyes diffuse away from the fusion site. If vesicles are labeled at non self-quenching concentration, fluorescence also decreases over time due to spreading of the fluorescent molecules but without a burst in the signal (Fig. 3C). Hemifusion is characterized by the increase in fluorescence signal of membrane dyes at self-quenching concentration that stays constant at this higher value. In this case, there is no change in signal from the vesicle interior. If the membrane is labeled at no self-quenching, the membrane signal decreases at nearly half of its initial fluorescence.

Using single-vesicle fusion, it was indeed shown that membrane fusion is a fast process that takes place within a few milliseconds after docking, as

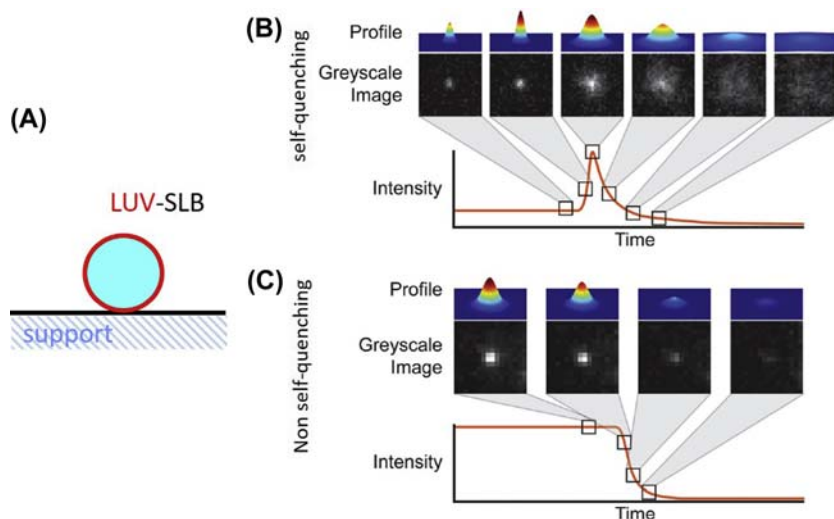


Fig.3 Outcomes of fusion of a small vesicle (LUV) and a supported lipid bilayer (SLB). (A) The vesicle contains a fluorescent lipid analog (red) and encapsulates a content marker (blue). The SLB to which the vesicle will fuse is represented in black. (B) Vesicle arrival and docking are observed as the appearance of a diffraction-limited spot (snapshots 1 and 2). If the vesicle is labeled (at the membrane or its interior) at self-quenching concentration, fusion results in a fluorescence bursting due to dequenching and the fluorescence vanishes as the molecules diffuse away. If label is not at self-quenching concentration, fusion results in simple decrease and diffusion of the fluorescence, as shown in (C). For B and C, the upper and mid rows represent signal from the vesicle and its brightness, whereas the bottom row shows the temporal changes in fluorescence. Adapted with permission from Ref. [134]. Copyright (2013) American Chemical Society.

probed both by lipid [70] and content mixing [71]. This finding showcases a very important advantage of the assay, and suggests that lipid mixing (or more rarely content mixing) is not the rate limiting step of fusion, as later demonstrated for SNARE liposomes [72]. This helps to explain why preincubating SNARE liposomes at non-physiological temperature increases lipid mixing [52]. A limitation of the method is that the membranes are in close contact with the support. This creates a very narrow gap of only a few nanometers between the membrane and the support that, (i) hinders the accommodation of lipids from the fusing vesicle, as well as (ii) the release of the content marker within this gap after fusion, and (iii) makes it practically impossible to control the membrane tension.

Some of the limitations above have been addressed by using a polymer cushion between the membrane and the support, thus increasing the gap

and decreasing the interactions. Rawle et al. ruptured giant vesicles with functionalized DNA onto a substrate functionalized with DNA of complementary antisense sequence, creating a ~ 8 nm gap between the bilayer and the solid surface [73]. Fusion (lipid and content mixing) was demonstrated for LUVs encapsulating self-quenching concentration of calcein. Analytical analysis of fluorescence dequenching confirmed the fluorescence bursting events are a result of content mixing rather than vesicle rupture above the bilayer. The DNA-mediated fusion had, nevertheless, a very low fusion efficiency, with only $\sim 6\%$ of docked LUVs undergoing full fusion. Later on, the authors hypothesized that having a DNA anchor that spans both leaflets might increase full fusion efficiency since the hybridized DNA would not diffuse away upon hemifusion, which presumably arrests most fusion events of DNA spanning one bilayer in the hemifusion state. This was confirmed by using DNA anchored by solanesol, a molecule long enough to span the whole bilayer [74]. Incorporation of solanesol increased the fraction of content mixing to $\sim 10\%$.

Fusion assays have also been used to characterize viral fusion. Enveloped viruses contain the viral particles enclosing the viral genome inside a bilayer envelope. It is only after fusion of the envelope with the target membrane that viruses release their content inside cells. A real-time influenza virus fusion with supported lipid bilayers formed on a polymer cushion revealed detailed kinetic intermediates for the hemifusion and fusion pore formation [75]. Influenza virus particles labeled at the lipid envelope and in its interior were immobilized in a microfluidic chamber that allows fast and complete solution exchange. Fusion was triggered by lowering the pH, which can also be accomplished by proton uncaging [76]. The pH change can be monitored by the changes in fluorescence of a pH-sensitive dye attached to the bilayer. SLB functionalized with ganglioside receptors enable virus binding. Later single-virus experiments showed that fusion kinetics (lipid mixing) is not influenced by receptor binding, and that binding does not produce receptor clustering [77]. Hemifusion was detected as the dequenching of a fluorescent lipid analog present in the virus envelope, and pore formation was detected from the release of the content dye. Kinetic information of the transition between fusion intermediates was obtained by computing the lag time between pH drop and hemifusion or full fusion for each virus particle. The analysis showed that the hemifusion is the rate-limiting step. Subsequent single-particle experiments further characterized the dynamics of fusion protein conformations that drive influenza virus fusion [78]. This assay also unraveled the ability of antibodies to stop viral

infection. The number of bound antibodies (Ab) to a single virion can be directly measured and it was used to determine the stoichiometry required to inhibit fusion (and hence infection) [79]. The number of bound Ab sufficient to inhibit fusion differs from different viral strains and the type of Ab, and vary from ~ 30 to 200 Ab/viral particle. In all cases, fusion is inhibited below saturation of the viral binding sites.

Vesicle fusion with supported bilayers formed on a polymer substrate demonstrated experimentally that membrane tension favors fusion [46]. Membrane tension on supported bilayers formed on a PDMS substrate was controlled by polymer stretching using a microfluidic chamber and was measured as the changes in area upon polymer stretching. Tension was found to increase the probability of membrane fusion, but this increase was not monotonic. While there seemed to exist a threshold above which fusion is promoted, additional increase in tension did not favor fusion further. Fusion efficiency was defined by the authors as the changes in fluorescence from the bilayer before vesicle addition to the condition after vesicle addition. Such measurements are semiquantitative; while they give information about fusion efficiency, it is not possible to quantify the number of fused vesicles, or conversely, how much membrane has been transferred. FRAP data confirmed the insertion of vesicle lipids in the membrane via fusion, but the measured diffusion was much lower than that found on free-standing bilayers due to the strong interaction of bilayer lipids with the substrate. Due to strong adhesion, a “tension-free state” was not accessible. Moreover, tension was not precisely assessed, although measuring the tension increments from the non-stressed state was feasible. Ideally, such experiments should be performed with free-standing bilayers (i.e. GUVs) in conditions where actual tension values can be measured, and if possible, controlled. Indeed, this is in principle possible using micropipette aspiration, although to the best of our knowledge, this has not been done yet.

It is also possible to minimize the interaction of membranes with a solid substrate by using a free-standing flat bilayer. Using pore-spanning membranes (PSMs), Kuhlmann et al. demonstrated the fusion of SNARE-reconstituted liposomes to the supported and free-standing areas of the PSM [80]. Vesicles bound to the pore-spanning part of the bilayer are fully mobile, whereas those bound to the substrate-bound part are immobilized. The authors explained the latter behavior as vesicle trapping by immobile SNARE proteins that are bound to the underlying support. Diffusing vesicles that move into the supported regions also become immobilized. After correcting for the docking probability and immobilization on the pore

rim, the probability of fusion is reduced by a factor of 2 in the free-standing regions, which was interpreted as being a result of higher SNARE concentrations in the supported regions due to immobilization. Relatively similar results were found with chromaffin granules fusing to PSMs [81].

5.2.2 Single-vesicle fusion with immobilized vesicles

In this assay, the incoming vesicles will fuse with other vesicles that are immobilized on a substrate (Fig. 4A). The immobilized vesicles are seen as static diffraction-limited spots. Typically, this assay is performed using FRET signal rather than simple changes in fluorescence intensity, which facilitates resolving the type of interactions the vesicles undergo. The vesicles are imaged at different wavelengths (different fluorescent channels) and the FRET signal is detected as the appearance of the acceptor fluorescence upon donor excitation (blue lines in Fig. 4B), whereas the incoming vesicle can be detected upon direct acceptor excitation (red line in Fig. 4B). If the FRET donor and acceptor are located on different membranes, docking would result in fluorescence co-localization with little or no changes in FRET (Fig. 4B). Upon hemifusion, an increase in FRET to an intermediate value is observed. If a water-soluble dye is also present, its fluorescence will remain constant as there is no content mixing. Full-fusion results in an increase in FRET to a higher level and this is followed by an increase in content mixing. The use of a content reporter (retained in the vesicle) inherently reports membrane integrity before and upon fusion, and thus it could be directly

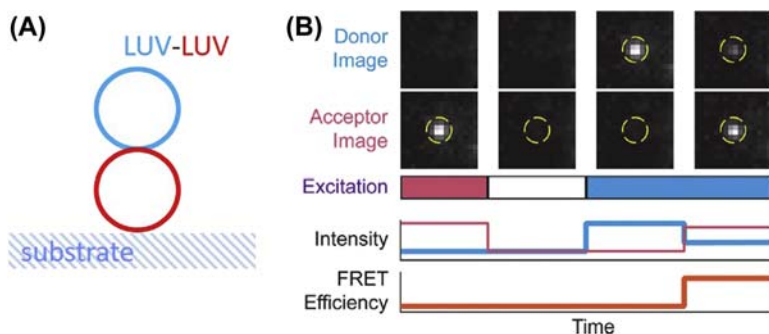


Fig.4 Outcomes of fusion of a small vesicle (LUV) with another one immobilized to a substrate. (A) Representation of the arrival of a fusing donor vesicle (blue) with an acceptor vesicle (red) that is immobilized on a substrate. (B) Vesicles can be detected by direct excitation of their respective dyes (first three rows), whereas the fusion intermediates are detected by changes in FRET (fourth and fifth rows). Adapted with permission from Ref. [134]. Copyright (2013) American Chemical Society.

checked whether fusion proceeds without membrane leakage. Therefore, the use of multiple dyes in combination with FRET allows to resolve membrane fusion intermediates in real time, to resolve the onset of fusion activation and to detect possible changes in membrane integrity that are associated to fusion.

This single vesicle-vesicle fusion assay was first reported by Yoon et al. [82] and later became one of the most popular single-vesicle fusion assays due to its simplicity and power. Single vesicles are immobilized to a support via ligand receptor interactions (i.e. biotin and streptavidin) and hundreds or thousands of individual diffraction-limited spots from vesicles are observed in a single field. In comparison to vesicle-SLB fusion, vesicle-vesicle fusion has the advantage that the fusing pair does not diffuse away from the field of view, and thus they could be observed for infinite amount of time. In Yoon et al., liposomes were reconstituted with yeast SNAREs, proteins that drive constitutive membrane fusion [82]. The authors were able to resolve for the first time, hemifusion, flickering of the fusion pore and to obtain kinetic data from the transition between fusion intermediates, as well as resolve the population fraction of vesicles that had undergone fusion. They were able to assign the measured FRET values to a fusion intermediate. This study paved the way for more complex single-vesicle membrane fusion studies. Using this assay, the same group characterized the role of the calcium-sensor syt on membrane fusion [83] and the regulatory role of complexin in SNARE-mediated membrane fusion [84]. Complexin was shown to enhance fusion of SNARE vesicles in the presence of syt and calcium, whereas it inhibits fusion with SNAREs alone [84]. Later, they combined the changes in FRET associated with lipid mixing to the use of a content mixing indicator for constitutive and regulated fusion. Whereas yeast SNAREs drive full fusion on their own [85], neuronal SNAREs alone trigger mainly hemifusion, and the rate of (hemi)fusion is much lower than in the presence of the regulatory proteins [86]. Further regulation of fusion is provided by complexin that aids the opening and expansion of the fusion pore [87].

5.2.3 Other single-vesicle systems

There are variations of the vesicle-flat membranes and the vesicle-vesicle fusion systems that are difficult to be classified into the definitions above. Early single-vesicle systems were based on the fusion of single liposomes (LUVs) with black lipid membranes (BLM) – a lipid bilayer suspended on a hole on a Teflon spacer that separates two aqueous compartments [88].

The fusion assay consists of detecting the changes in fluorescence and conductance from fusing lipid vesicles added to one side of the BLM (the *cis* side). Membrane interaction/adhesion is promoted by Ca^{2+} ions, and fusion is triggered by osmotic gradient [89]. The vesicles contain quenching concentrations of a fluorescent marker, and fluorescence bursting is an indication of lipid mixing. The vesicles also contain a porin molecule, whose insertion into the BLM upon full-fusion results in a detectable increase in conductance, which is used to detect content mixing. This method has the advantage that regulatory molecules could be easily added on either side of the fusing membranes, which is not feasible with other approaches. The addition of lipids with specific geometry on different membrane sides demonstrated how fusion intermediates are modulated by lipid geometry [89].

Single vesicle-vesicle fusion assays can also be performed without the need of vesicle immobilization. In that case, the fusing partners will be diffusing in solution. Vesicle diffusion and the changes in FRET associated with membrane fusion and fusion intermediates can be detected using fluorescence correlation and cross correlation spectroscopy (FCS and FCCS, respectively). The principle consists of detecting bursts in fluorescence from vesicles diffusing in and out of the confocal spot. FCS and FCCS also use FRET in order to detect fusion intermediates. Non interacting vesicles would diffuse unhindered and display the fastest diffusion. Docked vesicles would show cross correlation as they diffuse together, but without changes in FRET. Hemifused vesicles will also display co-diffusion, but FRET will increase. In both cases, diffusion will be slowed down due to the larger complex size. Full fused vesicles will display a higher FRET value. This approach was used to characterize the evolution of fusion for SNARE-reconstituted liposomes from docking at early incubation times, to fusion at later times [90]. In their assay, the authors also used fluorescence lifetime to characterize fusion. Due to FRET, fluorescence of FRET donors in the fused vesicles display a shorter lifetime. They also showed that liposome curvature (size) affects the rate of lipid mixing but not the rate of vesicle docking. A similar approach was used to characterize the role of the lipid PIP_2 on the fusion of SNARE vesicles under the regulation of *syt1* and calcium [91]. The authors demonstrated that without calcium, *syt1* increases the docking rate by three orders of magnitude by binding the SNARE complex and PIP_2 . Another study showed that the α -synuclein oligomers, but not monomers, efficiently inhibits SNARE-mediated membrane fusion (lipid mixing) by preventing SNARE complex formation [92]. All the

examples above make use of lipid mixing as a fusion readout, whereas content mixing is still to be demonstrated.

5.2.4 Outlook: single-vesicle studies

In summary, by allowing direct observation of individual particles, single-vesicle assays have the power to resolve the fate of the fusing membranes under the control of regulatory factors. The use of multiple fluorescent probes in different locations (membrane partners or aqueous compartments), in combination with different techniques, allows the detection of fusion intermediates and kinetic transitions that are not possible with ensemble methods. Because the interactions are observed in real time, there is no need for synchronization. Rare events are detectable and different populations can be readily identified. The need for immobile samples facilitates imaging and analysis, but more recent approaches also permit the detection of fusion without immobilization, although the demonstration of content mixing are still to be shown. The next step would be not only to detect membrane fusion and its intermediates and binding partners, as well as their role in the kinetics of fusion, but also to externally control and measure the changes in mechanical properties that are associated with fusion but inaccessible with sub-diffraction-limited vesicles due to their small size.

5.3 Giant vesicle fusion assays

The single-vesicle fusion assays reported in the previous section are based on the detection of fusion from the changes in membrane fluorescence of diffraction-limited spots, either from vesicles (mainly LUVs or SUVs) fusing to a flat membrane patch, or to other vesicles. These methods provide information about a vast range of parameters and enable fine spatial and temporal control of the fusion reaction. However, the membrane changes incurring from fusion are not directly detected and, in general, it is not possible to directly manipulate these vesicles and assess their state. With the merge of two membrane compartments, membrane fusion inevitably involves changes in membrane area and compartment volume [22]. Cells control the excess area of their membranes by the balance between membrane fusion and its opposite counterpart fission [93]. When membrane reservoirs (e.g. membrane stored in wrinkles and folds) are depleted, extra membrane can be mobilized to the plasma membrane by insertion from inner stores via exocytosis as observed upon the engulfment of large particles [94]. These local processes have global implications in the whole cell. In addition to tension, other mechanical parameters are known to be important in the course

of fusion, such as spontaneous curvature, and membrane fluidity. Therefore, studying fusion using membranes large enough to be visualized and that are amenable to mechanical manipulation can potentially increase the range of parameters that can be studied upon membrane fusion.

Giant unilamellar vesicles are an excellent model system to study membrane fusion. While their large size allows fusion to be directly observed under the microscope using very similar approaches used for small vesicles, they are also amenable to mechanical manipulation [33,34]. On the one hand, direct GUV observation has the potential to not only unravel different fusion intermediates and to resolve kinetics and dynamics of fusion that are afforded using small vesicles, but also to follow the local morphology of membranes and the global transformations of the whole vesicle as membranes fuse. On the other hand, direct manipulation of vesicles can provide information about the mechanical changes associated with fusion, such as changes in tension or elasticity. It is also possible to directly manipulate vesicles and study how fusion is regulated by membrane mechanics. In this section, we divide the use of GUVs as a model fusion system into two categories: (i) fusion between two GUVs and (ii) fusion between small vesicles and GUVs. As we shall see below, there are differences in either system that will make them more suitable for specific purposes.

5.3.1 GUV-GUV fusion

The fusion of GUVs to other GUVs have been speculated since the first reports of GUV formation more than 30 years ago [95]. It has been demonstrated that GUVs fuse as they form, and this has been hypothesized as one of the main mechanisms for vesicle growth [34,96,97]. Because membrane fusion is associated with a high energy barrier and therefore occurs with a very low rate [5], a number of approaches have been explored to induce GUV-GUV fusion, including the use of multivalent ions [98], ligand-mediated [99–101], peptide and SNARE-induced fusion [102,103], opposite charge [104,105], electrofusion [106], fusion initiated by optically heating nanoparticles [107,108] (see also Table 2 in Ref. [109] for a literature overview on electrofusion and laser-mediated fusion of vesicles and cells); some of these approaches will be discussed in more detail below.

When two GUVs fuse, it is possible to *see* the merging and mixing of their lipids and aqueous contents (see Fig. 5), which is only indirectly probed when using small vesicles. Two GUVs, from the same or different populations reconstituted with lipid dyes of different colors, can be brought into contact with the help of an alternating electric field i.e. dielectrophoresis

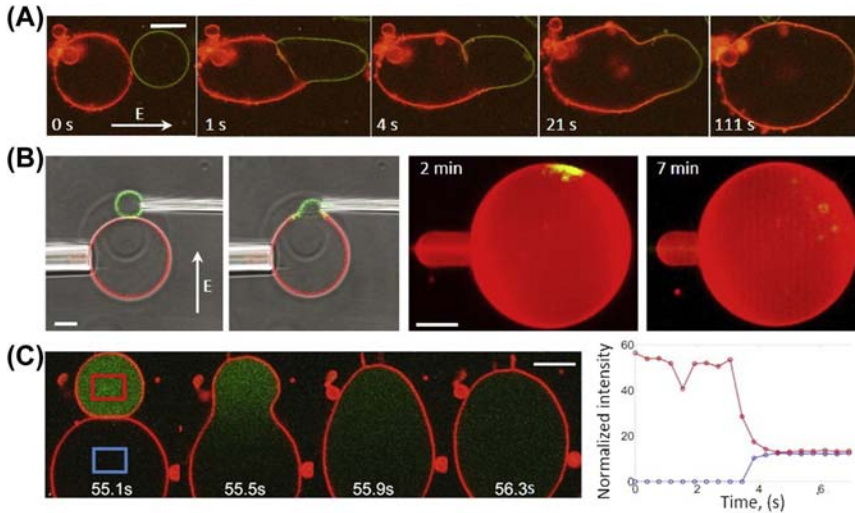


Fig.5 Lipid and content mixing in GUV-GUV fusion. Prior to fusion, the vesicles are brought in contact and aligned using AC electric field in (A), micropipette manipulation in (B), and optical trapping in (C). Fusion is triggered by an electric pulse (A, B) or nanoparticle optical heating (C). The field direction is indicated with an arrow. (A) Confocal scans of vesicles with similar membrane composition except for the lipid label, encapsulating 0.3 mM Na₂S (red) and 0.3 mM CdCl₂ (green) undergoing fusion. After fusion, fluorescence from the product (CdS quantum-dot-like nanoparticles) is detected in the interior of the fused vesicle. The fluorescence signal from the two membranes mixes over time. The time after applying the pulse is indicated on the micrographs. The scale bar is 20 μ m. Reproduced with permission from Ref. [116]. Copyright John Wiley and Sons. (B) Electrofusion of vesicles with different membrane composition as observed with phase-contrast overlaid with confocal cross sections (first two images) and confocal 3D projection (last two images). After application of an electric pulse (250 kV/m, 100 ms) the vesicles fuse to form a three-component vesicle in the single-phase region of the phase diagram of this lipid mixture. The lipids mix quickly after the fusion, as shown in the last two images. The scale bars correspond to 20 μ m. Reprinted from Ref. [113], Copyright (2013), with permission from Elsevier. (C) Confocal images of the fusion process of two GUVs, one of which contains only a sucrose solution, the other sucrose mixed with calcein (green). The scale bar is 10 μ m. Intensity emitted by calcein in the two boxed regions in the first image, red trace (from red box) is from a region that starts out being inside the calcein-containing vesicle, blue trace (from blue box) is from a region that starts out being in the empty vesicle. Approximately \sim 0.3–0.5 s after fusion the calcein intensity distribution is uniform within the fused GUV. Adapted with permission from Ref. [107]. Copyright (2015) American Chemical Society.

[106,110] (see also Chapter 15 by Dimova and Riske in Ref. [34]), by applying a flow and immobilizing them in microfluidic traps [111], optical trapping [107], micropipette manipulation [112,113]. A content marker can be encapsulated in one of the populations to check for full fusion

(Fig. 5C). When two GUVs fuse, it is possible to directly observe the fusion of their membranes and mixing of their internal contents. At the end of the experiment, the fused GUV is larger, intact and some membrane excess is often stored as internal or external structures such as buds and tubes. Therefore, by using GUVs, it is possible to observe fusion and the morphological transformations associated.

Since reconstituting fusion proteins in GUVs is challenging, most fusion experiments have been carried out using other fusogens. Already 20 years ago, MacDonald and coworkers used electrically charged GUVs to induce membrane fusion [104,105]. They showed that GUVs dock at low membrane charge and this does not result in vesicle leakage. Increasing charge leads to hemifusion and the exchange of lipids in the outer leaflet among the (hemi)fused GUVs, and this is the end state of fusion. As expected from the stalk hypothesis, cone-shape lipids were observed to favor hemifusion. Further increasing the charge led to full fusion. Similarly to fusion with small vesicles, GUV-GUV fusion was shown to be very fast (<33 ms). Interestingly, the fully fused GUVs seemed not much bigger than the two individual vesicles before fusion, but they do display bright fluorescent buds. Hence the gained area via fusion is stored as curved structures.

Membrane fusion intermediates that precede fusion have been observed using GUVs. Sun et al. used hemifused GUVs to study the energy of adhesion and hemifusion of membranes [114]. GUVs adhesion and hemifusion was induced by lowering pH, polymer osmotic depletion or lipid cross-bridging using cationic peptides. Hemifusion was confirmed from the exchange of lipids from the outer leaflet only without content mixing (Fig. 6A). From the shape of the hemifused GUVs and the length of the adhesion area and the membrane tension assessed with the help of micropipette aspiration (Fig. 6B), they determine the adhesion energy for weakly and strongly interacting membranes, which can vary by two orders of magnitude. Using DNA-functionalized lipids, Heuvingh et al. detected mainly adhesion and hemifusion between two GUVs, but also full fusion [100]. As observed with small vesicles, DNA-mediated interactions result in low degree of full fusion, with only $\sim 5\%$ of the vesicle pairs fully fusing. The hemifusion diaphragm has also been observed in more biologically-relevant context. In the presence of divalent cations, GUVs containing the transmembrane domains of fusion peptides (TMDs) were made to adhere and (hemi)fuse with non-functionalized GUVs [51]. Hemifusion was observed as lipid depletion in the adhesion zone and exchange of outer leaflet lipids (Fig. 6C). After hemifusion, the dye redistributes into the

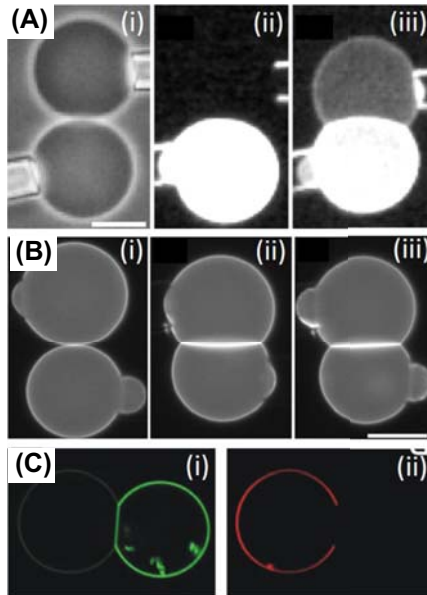


Fig. 6 GUV-GUV hemifusion. (A) Two GUVs aspirated micropipettes are induced to interact in the presence of PEG and at pH 4; (i) phase contrast image, (ii, iii) epifluorescence signal. Hemifusion is observed as the exchange of lipid (iii) without content mixing (ii). (B) Hemifusion induced by an HIV peptide: (i) before introducing the peptide the vesicles do not adhere, and after the peptide is introduced (ii, iii) adhesion is observed. The vesicle tension, controlled by the micropipette aspiration, modulates the area of the adhesion zone. Note that the increase in aspirating pressure (observed as an increase in the projected area inside the pipette) decreases the size of the adhered region. Scale bars in (A, B) correspond to $25\ \mu\text{m}$. (A) and (B) are reprinted from Ref. [114], Copyright (2011), with permission from Elsevier. (C) Hemifused GUVs as observed by lipid exchange (green) from one vesicle to the other (i). The transmembrane peptide that spans both bilayers (red) does not redistribute to the membrane of the left GUV in (ii). Reprinted from Ref. [51], Copyright (2010), with permission from Elsevier.

hemifused vesicles, see Fig. 6C(i). Since the transmembrane peptides span both leaflets, they do not redistribute into the hemifusion diaphragm, see Fig. 6C(ii).

Single (small) vesicle studies have demonstrated in many instances that membrane fusion is a very fast process. Using optical microscopy and high-speed imaging, Haluska et al. fused two individual GUVs to characterize the speed of membrane fusion and the expansion of the pore fusion neck [101]. Fusion was induced either by ligand-receptor interactions or electroporation. The authors showed that the opening of the fusion neck

is extremely fast, in the order of cm/s. With this speed, the formation of the neck occurs in nanoseconds. Fusion pore neck expansion displays two kinetic regimes, fast opening in the order of μs that is driven by membrane tension, and, at a later stage, a slower one (in the order of seconds) that is related to the displacement of the fluid inside and around the vesicles and to the membrane elasticity. For small vesicles, only the former is relevant. Fusion results in the increase in vesicle area, and the excess of membrane acquired during fusion can result in both membrane fluctuations and the formation buds. GUV fusion can also be used in biotechnology. The mixing of the membranes can create vesicles with controlled membrane compositions [106,113], whereas mixing of aqueous volumes can be used for the controlled synthesis of nanoparticles inside GUVs microreactors [115,116], as shown also in Fig. 5. GUVs have been also successfully fused with cells, see e.g. Refs. [108,110,112,117,118], and plasma membrane derived vesicles [109].

5.3.2 Small vesicle-GUV fusion

At the molecular scale, fusion of two membranes should be independent of their sizes, except that the highly curved membranes of small vesicles (i.e. SUVs or LUVs) display two features important in the context of fusion: they can be tense due to curvature stress and they display an asymmetry in the number of lipids on their leaflets, with more lipids in their outer leaflet. It is possible to study the effects of membrane curvature, by fusing LUVs of different sizes with GUVs. The fusion of SUVs or LUVs with GUVs mimics the topology of intracellular vesicles fusing with the plasma membrane. Small vesicle-GUV fusion assays are easier to perform since the small vesicles can reach the GUVs by simple diffusion, without the need of external manipulation to bring them in contact. Thus, the fusion of many small vesicles with a single GUV is straightforward. In fact, here fusion efficiency can be assessed from estimating the number of fusing small vesicles offering higher statistics, which is not feasible with the low throughput GUV-GUV fusion assay.

The role of SNARE proteins on LUV-GUV fusion was studied by Witkowska and Jahn [119]. SNARE proteins reconstituted in GUVs were mobile. Fusion of small vesicles containing synaptobrevin, or the fusion of chromaffin granules purified from bovine adrenal granules with GUVs containing complementary t-SNAREs was probed by acceptor photobleaching FRET — bleaching of acceptor dyes transferred from the LUVs increased donor fluorescence. Content mixing using self-quenching concentration

of calcein was also tested. However, from the images, it is not very clear whether the content was transferred from the LUVs to the GUVs (presumably, the dye in excess was not removed), and it was not demonstrated that fusion proceeds leakage-free (which could defile the content mixing signal). Fusion efficiency was presumably very low judging from the weak lipid transfer and this should be a consequence of the very low docking observed. The results are somehow in agreement with data from bulk and single-vesicle experiments, in which SNAREs alone are not very fusogenic. Other studies also showed that fusion with SNAREs only increases with an increase in GUV tension, similarly to observations on PSMs [46] as discussed above. There is also a threshold in GUV tension, above which fusion is promoted and stabilized. These experiments are important because fusion takes place with the free-standing membranes of the GUVs, although the GUV vesicles are strongly adhered to a surface. It was, nevertheless, not possible to truly quantify fusion efficiency since the measurements are based on relative changes in fluorescence.

In order to investigate the role of accessory fusion proteins, Tareste et al. studied the fusion of LUVs (~ 100 nm) and GUVs using SNARE proteins in the absence and presence of Munc18 [103]. In cells, v-SNAREs are present in the small vesicles, whereas t-SNAREs are present in the plasma membrane [41]. In the employed assay, the SNARE topological distribution was the opposite, possibly due to technical issues. v-SNARE proteins reconstituted in the GUVs were shown to undergo free diffusion, which is presumably required for fusion. Soluble t-SNARE proteins bound v-SNARE in the GUV membrane, and binding was enhanced in the presence of Munc18. By observing GUVs, it was possible to detect single small vesicles docking to the GUV surface and fusing. Fusion was probed by transfer of lipids from the LUVs to the GUVs. LUVs fused with the GUVs, and fusion was enhanced by Munc18 as a consequence of increased binding, thus again suggesting that docking is the rate-limiting step. From a calibration curve with increasing lipid dye concentration, fluorescence intensity in the membrane was measured as a function of dye signal. The measured intensity in the GUVs after fusion with small vesicles was used to calculate the number of vesicles that had fused, and thus, the true fusion efficiency could be measured. Fusion efficiency is shown to increase with incubation time, and efficiency increases with Munc18 concentration. In the most efficient conditions, 10–40 LUVs fuse with a single GUV of 10 μm in diameter. Reliable fusion of SNARE proteins and GUVs using content mixing has not yet been demonstrated.

Membrane fusion involves large structural rearrangements of the lipid bilayer. These rearrangements are inhibited in more rigid membranes, such as those rich in cholesterol [6,7]. Yet, the fusion of HIV viruses to cellular membranes is promoted by cholesterol (Chol). This apparent contradiction was reconciled by Yang et al., who showed that virus-like particles bind preferentially the lipid domain interface in phase-separated, Chol-rich membranes [120]. The affinity for the domain interface is a general process as it was observed with supported lipid bilayers, GUVs and vesicles derived from living cells, but specific to HIV-like virus [121]. In SLB, particle binding to the domain interface also promoted hemi- and full fusion, although fusion with GUVs was rather inefficient. Later, the same team demonstrated that the increased affinity for the domain interface is related to the domain line tension, the energy penalty of frustrating lipids at the domain interface due to hydrophobic mismatch [122]. Using SLB (but not GUVs), they showed that membrane fusion (content mixing) is a linear function of line tension. Their observations are very important and rather general, demonstrating that the hydrophobic mismatch, but not the lipid type, is important for virus binding and fusion.

Other membrane material properties are also important for membrane fusion and fusion intermediates. Recent high-resolution cryoelectron microscopy studies revealed a new intermediate on the pathway to fusion. In the stalk hypothesis, a single bilayer is formed from the contact of the distal monolayers of the opposing membranes, where the fusion pore is formed [7]. In this case, full fusion occurs with no leakage of their contents. However, recent experimental evidence from small vesicles showed that the membrane may rupture forming a pore “outside” the hemifusion diaphragm, and these pores were shown to be stable, leading to the leakage of membrane contents [123]. Haldar et al. studied the role of membrane spontaneous curvature on membrane rupture followed by fusion [124]. They used lipid-labeled influenza virus-like particles incubated with GUVs in the presence of a solution containing a small water-soluble probe. Membrane fusion was detected from the transfer of fluorescence lipids from the LUVs to the GUVs, whereas GUV pores were detected as the entry of a water-soluble dye present (in the medium) into the GUVs. They found that the fraction of porated GUVs depends on membrane curvature, and this is a universal behavior that is independent of the specific membrane composition. Membranes containing lipids at different fractions but similar overall (negative) curvature displayed a similar fraction of permeable vesicles.

The above reports mimic membrane fusion using fusion proteins of virus and virus-like particles, but fusion efficiency in all cases is very low. Other non-natural fusogens can be used to boost fusion. Trier et al. used pH-sensitive liposomes containing the negatively charge lipid oleic acid (OA) and the negatively curved lipid DOPE (dioleoylphosphatidylethanolamine) [125]. These liposomes are stable at high pH, but neutralization of OA at acidic pH destabilizes the vesicles. OA:DOPE liposomes were induced to fuse with neutral and positively charged GUVs. Small liposomes contained a FRET acceptor membrane dye, whereas the GUVs contained a donor FRET dye, and fusion (lipid mixing) was detected by FRET. Alternatively, the liposomes were also prepared with encapsulated calcein at a self-quenching concentration to detect full-fusion (content mixing). At pH 9.5, the LUVs neither docked nor fused with the GUVs, whereas at pH 6.1, extensive fusion was observed (Fig. 7A,B). In a separate experiment,

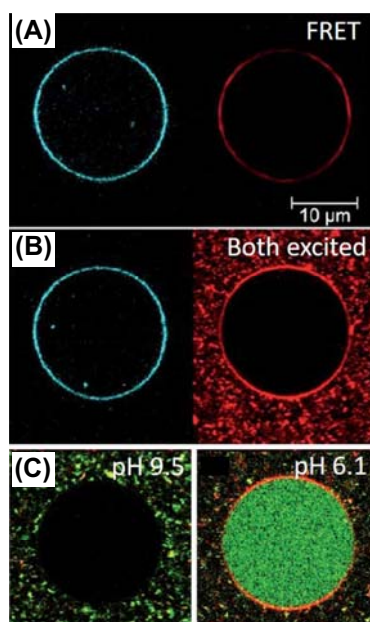


Fig.7 pH-mediated membrane fusion. OA:DOPE LUVs fuse with positively-charged GUVs (see main text for details). (A) Direct GUV excitation (left) and FRET (right) show that LUV lipids were transferred to the GUVs via membrane fusion. (B) Direct excitation of both GUV (left) and LUV lipids (right), to allow identification of LUVs. (C) Full fusion (content mixing) at low but not high pH is demonstrated with calcein signal (green) encapsulated in the LUVs and transferred to the GUV interior. Adapted from Ref. [125] with permission from The Royal Society of Chemistry.

content mixing is also observed for these conditions (Fig. 7C). Membrane fusion was charge-dependent, and LUV incubation with neutral GUVs at lower pH did not lead to fusion. Efficiency was assessed from calibration curves for the lipid and content dyes. Both methods produced very consistent results, with ~ 800 LUVs fusing with a GUV of 10 μm in diameter, thus two order of magnitude higher than when fusion is induced by SNARE proteins. Charge-mediated membrane fusion was used by Biner et al. to deliver proteins from LUVs–reconstituted membrane to GUVs [126]. The proton pump bo_3 oxidase and the ATP-producing ATP-synthase were efficiently reconstituted into GUVs upon fusion-mediated delivery and demonstrated to be active. The method is rather general and other proteins can be included, although their activity needs to be tested individually. Protein reconstitution into GUVs after fusion with protein-containing LUVs have also been demonstrated after peptide-induced fusion [102,127], and the transferred proteins were also shown to be functional. Thus, high fusion efficiency can be achieved using synthetic fusogens and this can have a large impact in biotechnological applications.

More recently, we have thoroughly characterized fusion of charged LUVs and GUVs [128]. Positively charged LUVs with fusogenic properties [129,130] were incubated with GUVs of increasing charge density. GUV charge was controlled by increasing the fraction of charged lipids from 0 to 100 mol%. GUVs were initially green (false color) and LUVs were red, and fusion was detected by the changes in GUV color. In agreement with GUV-GUV fusion, LUVs dock and hemifuse with GUVs when the GUV surface charge is low (Fig. 8A). The large number of hemifused LUVs results in asymmetric transfer of lipids to the outer leaflet of the GUVs versus no lipid contributed to the inner leaflet. This gives rise to stretching of the inner leaflet and frustration of the membrane, that eventually leads to GUV rupture. In contrast, LUVs fuse very efficiently with more negatively charged GUVs (Fig. 8B). Efficient fusion results in change in color from green to red and a very large increase in GUV area, observed by increased fluctuations. When too many LUVs fuse, GUV fluctuations are suppressed and the gained area is stored in the formed outward structures such as buds and tubes (Fig. 8B). Because fusion is shown to be leakage-free, the LUVs area asymmetry is attributed to the GUVs, and the excess of lipids in the outer leaflets gives rise to non-negligible spontaneous tension originating from the spontaneous curvature. As demonstrated

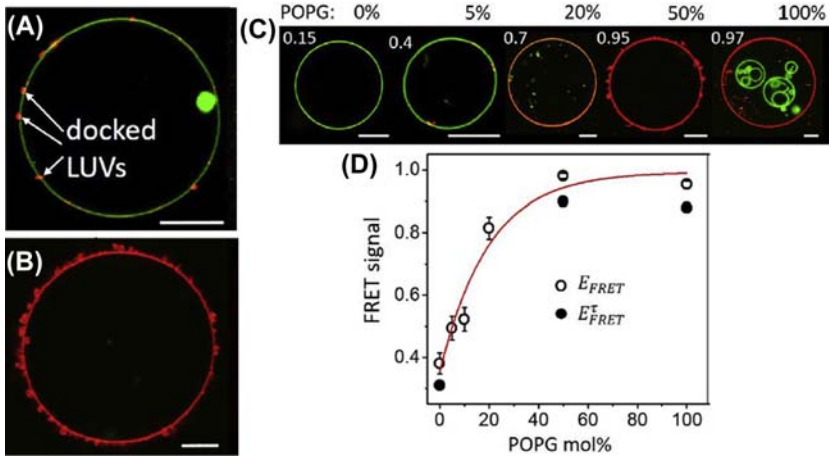


Fig.8 Highly efficient charge-mediated membrane LUV-GUV fusion. (A) Docking of LUVs (red) to a GUV (green) at low GUV charge. (B) At high GUV charge, fusion is very efficient and results in changing the GUV color and increasing its area (excess area is stored in the form of curved structures). (C) Fusion efficiency increases with increase in the fraction of the charged lipid in the GUV (POPG, palmitoylphosphatidylglycerol). The mole fraction of POPG is indicated above the images. The numbers indicated on the confocal cross sections correspond to the measured FRET values. (D) FRET signal as a function of POPG fraction as measured by intensity (open circles) and lifetime-based FRET (solid circles). Reprinted from Ref. [128], Copyright (2019), with permission from Elsevier.

in other studies [131,132], weak alternating electric fields can be applied to pull and assess the excess area in early stages of fusion (or alternatively at lower LUV concentration), but it is unable to pull the area stored in tubes, demonstrating significant tension. The observations above are very important as the type of interaction (i.e. hemifusion or full fusion) can be inferred from the changes in GUV morphology. From a FRET calibration curve, it is possible to quantify the true fusion efficiency, which was converted into number of lipids transferred to a single GUV. For large enough GUVs, over a hundred thousand LUVs can be fused, which represents the most efficient fusion system ever reported. From the FRET calibration, we were able to determine of GUV final composition at the single vesicle level. Fusion occurs until the charges are saturated. Presumably, this is also the case with fusogenic molecules, in which the exhaustion of the fusogen will stop the fusion reaction. Microfluidics experiments permitted real-time observations of a GUV fusing with many LUVs, and the kinetics of fusion could be directly assessed.



6. Conclusions

In this review, we have provided a concise description of the main membrane model systems (submicron liposomes, giant unilamellar vesicles and supported lipid bilayers) and the main assays actively employed in investigating fusion processes. The different methods provide different information that is often complementary and they vary in their complexity. The review is meant as an introduction for newcomers, but also contains critical remarks for experienced researchers in the field of membrane fusion, emphasizing the main properties but also some drawbacks of the model systems and of the experimental assay. For example, the imprecise and often very different definition of fusion efficiency in bulk methods hinders direct comparison with assays where single fusion events can be detected, and hence, the effects of fusogens on membrane fusion is more difficult to compare. We have also reviewed major findings in the literature obtained from these models and assays regarding the mechanisms of fusion, the role of individual proteins and regulatory mechanisms, as well as physical properties of membrane that govern it. The assays described here have proven extremely valuable in revealing the molecular and biophysical features and determinants regulating fusion. Combined, they permit the collection of mechanistic, kinetic, morphological and mechanical data down to the level of a single interacting fusion partner under well-defined and controlled conditions.

Acknowledgments

This work was a part of the MaxSynBio consortium, which was jointly funded by the Federal Ministry of Education and Research of Germany (BMBF) and the Max Planck Society (MPG). We thank R. Lipowsky for critically reading the manuscript and for the constructive comments.

References

- [1] W. Wickner, R. Schekman, Membrane fusion, *Nat. Struct. Mol. Biol.* 15 (2008) 658–664.
- [2] R. Jahn, T. Lang, T.C. Sudhof, Membrane fusion, *Cell* 112 (2003) 519–533.
- [3] S.C. Harrison, Viral membrane fusion, *Nat. Struct. Mol. Biol.* 15 (2008) 690.
- [4] Y.A. Chen, R.H. Scheller, SNARE-mediated membrane fusion, *Nat. Rev. Mol. Cell Biol.* 2 (2001) 98–106.
- [5] S. Martens, H.T. McMahon, Mechanisms of membrane fusion: disparate players and common principles, *Nat. Rev. Mol. Cell Biol.* 9 (2008) 543–556.
- [6] L. Chernomordik, M.M. Kozlov, J. Zimmerberg, Lipids in biological membrane fusion, *J. Membr. Biol.* 146 (1995) 1–14.
- [7] L.V. Chernomordik, M.M. Kozlov, Mechanics of membrane fusion, *Nat. Struct. Mol. Biol.* 15 (2008) 675–683.

- [8] J. Rizo, T.C. Südhof, Mechanics of membrane fusion, *Nat. Struct. Biol.* 5 (1998) 839–842.
- [9] J.C. Shillcock, R. Lipowsky, Tension-induced fusion of bilayer membranes and vesicles, *Nat. Mater.* 4 (2005) 225–228.
- [10] A. Grafmüller, J. Shillcock, R. Lipowsky, Pathway of membrane fusion with two tension-dependent energy barriers, *Phys. Rev. Lett.* 98 (2007).
- [11] A. Grafmüller, J. Shillcock, R. Lipowsky, The fusion of membranes and vesicles: pathway and energy barriers from dissipative particle dynamics, *Biophys. J.* 96 (2009) 2658–2675.
- [12] L. Gao, R. Lipowsky, J. Shillcock, Tension-induced vesicle fusion: pathways and pore dynamics, *Soft Matter* 4 (2008) 1208–1214.
- [13] Y.G. Smirnova, S.-J. Marrink, R. Lipowsky, V. Knecht, Solvent-exposed tails as pre-stalk transition states for membrane fusion at low hydration, *J. Am. Chem. Soc.* 132 (2010) 6710–6718.
- [14] C. Allolio, A. Magarkar, P. Jurkiewicz, K. Baxová, M. Javanainen, P.E. Mason, R. Šachl, M. Cebecauer, M. Hof, D. Horinek, V. Heinz, R. Rachel, C.M. Ziegler, A. Schröfel, P. Jungwirth, Arginine-rich cell-penetrating peptides induce membrane multilamellarity and subsequently enter via formation of a fusion pore, *Proc. Natl. Acad. Sci.* 115 (2018) 11923.
- [15] L. Yang, H.W. Huang, Observation of a membrane fusion intermediate structure, *Science* 297 (2002) 1877.
- [16] S. Sharma, M. Lindau, The mystery of the fusion pore, *Nat. Struct. Mol. Biol.* 23 (2016) 5.
- [17] J.B. Sørensen, Conflicting views on the membrane fusion machinery and the fusion pore, *Annu. Rev. Cell Dev. Biol.* 25 (2009) 513–537.
- [18] A. Chanturiya, L.V. Chernomordik, J. Zimmerberg, Flickering fusion pores comparable with initial exocytotic pores occur in protein-free phospholipid bilayers, *Proc. Natl. Acad. Sci. U. S. A.* 94 (1997) 14423–14428.
- [19] N. Takahashi, T. Kishimoto, T. Nemoto, T. Kadowaki, H. Kasai, Fusion pore dynamics and insulin granule exocytosis in the pancreatic islet, *Science* 297 (2002) 1349.
- [20] R.M. Wightman, C.L. Haynes, Synaptic vesicles really do kiss and run, *Nat. Neurosci.* 7 (2004) 321–322.
- [21] H.-C. Chiang, W. Shin, W.-D. Zhao, E. Hamid, J. Sheng, M. Baydyuk, P.J. Wen, A. Jin, F. Momboisse, L.-G. Wu, Post-fusion structural changes and their roles in exocytosis and endocytosis of dense-core vesicles, *Nat. Commun.* 5 (2014) 3356.
- [22] I. Ivanov, R.B. Lira, T.Y.D. Tang, T. Franzmann, A. Klosin, L.C. da Silva, A. Hyman, K. Landfester, R. Lipowsky, K. Sundmacher, R. Dimova, Directed growth of biomimetic microcompartments, *Adv. Biosys.* 3 (2019) 1800314.
- [23] T.C. Südhof, Neurotransmitter release: the last millisecond in the life of a synaptic vesicle, *Neuron* 80 (2013) 675–690.
- [24] S.O. Rizzoli, Synaptic vesicle recycling: steps and principles, *EMBO J.* 33 (2014) 788.
- [25] A.D. Bangham, M.M. Standish, J.C. Watkins, Diffusion of univalent ions across lamellae of swollen phospholipids, *J. Mol. Biol.* 13 (1965) 238–8.
- [26] F. Szoka, D. Papahadjopoulos, Comparative properties and methods of preparation of lipid vesicles (liposomes), *Annu. Rev. Biophys. Bioeng.* 9 (1980) 467–508.
- [27] O. López, M. Cócera, R. Pons, N. Azemar, A. de la Maza, Kinetic studies of liposome solubilization by sodium dodecyl sulfate based on a dynamic light scattering technique, *Langmuir* 14 (1998) 4671–4674.
- [28] S.W. Hell, S.J. Sahl, M. Bates, X. Zhuang, R. Heintzmann, M.J. Booth, J. Bewersdorf, G. Shtengel, H. Hess, P. Tinnefeld, A. Honigsmann, S. Jakobs, I. Testa, L. Cognet, B. Lounis, H. Ewers, S.J. Davis, C. Eggeling, D. Klenerman,

- K.I. Willig, G. Vicidomini, M. Castello, A. Diaspro, T. Cordes, The 2015 super-resolution microscopy roadmap, *J. Phys. D Appl. Phys.* 48 (2015) 443001.
- [29] S.M. Christensen, D. Stamou, Surface-based lipid vesicle reactor systems: fabrication and applications, *Soft Matter* 3 (2007) 828–836.
- [30] R. Dimova, S. Aranda, N. Bezlyepkina, V. Nikolov, K.A. Riske, R. Lipowsky, A practical guide to giant vesicles. Probing the membrane nanoregime via optical microscopy, *J. Phys. Condens. Matter* 18 (2006) S1151–S1176.
- [31] P. Walde, K. Cosentino, H. Engel, P. Stano, Giant vesicles: preparations and applications, *Chembiochem* 11 (2010) 848–865.
- [32] R. Dimova, Giant vesicles: a biomimetic tool for membrane characterization, in: A. Iglič (Ed.), *Advances in Planar Lipid Bilayers and Liposomes*, Academic Press, Burlington, 2012, pp. 1–50.
- [33] R. Dimova, Giant vesicles and their use in assays for assessing membrane phase state, curvature, mechanics, and electrical properties, *Annu. Rev. Biophys.* 48 (2019) 93–119.
- [34] R. Dimova, C. Marques, *The Giant Vesicle Book*, Taylor & Francis Group, LLC, Boca Raton, 2019.
- [35] T. Robinson, Microfluidic handling and analysis of giant vesicles for use as artificial cells: a review, *Adv. Biosys.* 0 (2019) 1800318.
- [36] M. Przybylo, J. Sykora, J. Humpolickova, A. Benda, A. Zan, M. Hof, Lipid diffusion in giant unilamellar vesicles is more than 2 times faster than in supported phospholipid bilayers under identical conditions, *Langmuir* 22 (2006) 9096–9099.
- [37] M.L. Wagner, L.K. Tamm, Tethered polymer-supported planar lipid bilayers for reconstitution of integral membrane proteins: silane-polyethyleneglycol-lipid as a cushion and covalent linker, *Biophys. J.* 79 (2000) 1400–1414.
- [38] H. Pace, L. Simonsson Nyström, A. Gunnarsson, E. Eck, C. Monson, S. Geschwindner, A. Snijder, F. Höök, Preserved transmembrane protein mobility in polymer-supported lipid bilayers derived from cell membranes, *Anal. Chem.* 87 (2015) 9194–9203.
- [39] T.D. Lazzara, C. Carnarius, M. Kocun, A. Janshoff, C. Steinem, Separating attoliter-sized compartments using fluid pore-spanning lipid bilayers, *ACS Nano* 5 (2011) 6935–6944.
- [40] M. Weiss, J.P. Frohnmayer, L.T. Benk, B. Haller, J.-W. Janiesch, T. Heitkamp, M. Borsch, R.B. Lira, R. Dimova, R. Lipowsky, E. Bodenschatz, J.-C. Baret, T. Vidakovic-Koch, K. Sundmacher, I. Platzman, J.P. Spatz, Sequential bottom-up assembly of mechanically stabilized synthetic cells by microfluidics, *Nat. Mater.* 17 (2018) 89–96.
- [41] R. Jahn, R.H. Scheller, SNAREs - engines for membrane fusion, *Nat. Rev. Mol. Cell Biol.* 7 (2006) 631–643.
- [42] B.R. Lentz, PEG as a tool to gain insight into membrane fusion, *Eur. Biophys. J.* 36 (2007) 315–326.
- [43] J. Wilschut, D. Papahadjopoulos, Ca²⁺-induced fusion of phospholipid vesicles monitored by mixing of aqueous contents, *Nature* 281 (1979) 690–692.
- [44] U. Zimmermann, J. Vienken, Electric field-induced cell-to-cell fusion, *J. Membr. Biol.* 67 (1982) 165–182.
- [45] Z.T. Graber, Z. Shi, T. Baumgart, Cations induce shape remodeling of negatively charged phospholipid membranes, *Phys. Chem. Chem. Phys.* 19 (2017) 15285–15295.
- [46] T.-T. Kliesch, J. Dietz, L. Turco, P. Halder, E. Polo, M. Tarantola, R. Jahn, A. Janshoff, Membrane tension increases fusion efficiency of model membranes in the presence of SNAREs, *Sci. Rep.* 7 (2017) 12070.

- [47] K. Stebelska, P.M. Dubielecka, A.F. Sikorski, The effect of PS content on the ability of natural membranes to fuse with positively charged liposomes and lipoplexes, *J. Membr. Biol.* 206 (2005) 203–214.
- [48] C.G. Schuette, K. Hatsuzawa, M. Margittai, A. Stein, D. Riedel, P. Küster, M. König, C. Seidel, R. Jahn, Determinants of liposome fusion mediated by synaptic SNARE proteins, *Proc. Natl. Acad. Sci. U. S. A* 101 (2004) 2858.
- [49] J.M. Hernandez, A. Stein, E. Behrmann, D. Riedel, A. Cypionka, Z. Farsi, P.J. Walla, S. Raunser, R. Jahn, Membrane fusion intermediates via directional and full assembly of the SNARE complex, *Science* 336 (2012) 1581.
- [50] Y. Yang, P. Heo, B. Kong, J.-B. Park, Y.-H. Jung, J. Shin, C. Jeong, D.-H. Kweon, Dynamic light scattering analysis of SNARE-driven membrane fusion and the effects of SNARE-binding flavonoids, *Biochem. Biophys. Res. Commun.* 465 (2015) 864–870.
- [51] J. Nikolaus, M. Stöckl, D. Langosch, R. Volkmer, A. Herrmann, Direct visualization of large and protein-free hemifusion diaphragms, *Biophys. J.* 98 (2010) 1192–1199.
- [52] T. Weber, B.V. Zemelman, J.A. McNew, B. Westermann, M. Gmachl, F. Parlati, T.H. Sollner, J.E. Rothman, SNAREpins: minimal machinery for membrane fusion, *Cell* 92 (1998) 759–772.
- [53] M. Kyoung, Y. Zhang, J. Diao, S. Chu, A.T. Brunger, Studying calcium-triggered vesicle fusion in a single vesicle-vesicle content and lipid-mixing system, *Nat. Protoc.* 8 (2012) 1.
- [54] D. Hoekstra, T. De Boer, K. Klappe, J. Wilschut, Fluorescence method for measuring the kinetics of fusion between biological membranes, *Biochemistry* 23 (1984) 5675–5681.
- [55] D.K. Struck, D. Hoekstra, R.E. Pagano, Use of resonance energy-transfer to monitor membrane-fusion, *Biochemistry* 20 (1981) 4093–4099.
- [56] N. Duzgunes, T.M. Allen, J. Fedor, D. Papahadjopoulos, Lipid mixing during membrane aggregation and fusion: why fusion assays disagree, *Biochemistry* 26 (1987) 8435–8442.
- [57] J. Wilschut, N. Duzgunes, R. Fraley, D. Papahadjopoulos, Studies on the mechanism of membrane fusion: kinetics of calcium ion induced fusion of phosphatidylserine vesicles followed by a new assay for mixing of aqueous vesicle contents, *Biochemistry* 19 (1980) 6011–6021.
- [58] W.C. Tucker, T. Weber, E.R. Chapman, Reconstitution of Ca²⁺-regulated membrane fusion by synaptotagmin and SNAREs, *Science* 204, 304, 435.
- [59] G. van den Bogaart, M.G. Holt, G. Bunt, D. Riedel, F.S. Wouters, R. Jahn, One SNARE complex is sufficient for membrane fusion, *Nat. Struct. Mol. Biol.* 17 (2010) 358.
- [60] M.C. Chicka, E. Hui, H. Liu, E.R. Chapman, Synaptotagmin arrests the SNARE complex before triggering fast, efficient membrane fusion in response to Ca²⁺, *Nat. Struct. Mol. Biol.* 15 (2008) 827.
- [61] Z. Wang, H. Liu, Y. Gu, E.R. Chapman, Reconstituted synaptotagmin I mediates vesicle docking, priming, and fusion, *J. Cell Biol.* 195 (2011) 1159.
- [62] M. Zick, C. Stroupe, A. Orr, D. Douville, W.T. Wickner, Membranes linked by trans-SNARE complexes require lipids prone to non-bilayer structure for progression to fusion, *eLife* 3 (2014) e01879.
- [63] Y. Lai, L. Zhao, B. Bu, X. Lou, D. Li, B. Ji, J. Liu, J. Diao, Y.-K. Shin, Lipid molecules influence early stages of yeast SNARE-mediated membrane fusion, *Phys. Biol.* 12 (2015) 025003.
- [64] V.J. Starai, Y. Jun, W. Wickner, Excess vacuolar SNAREs drive lysis and Rab bypass fusion, *Proc. Natl. Acad. Sci.* 104 (2007) 13551.

- [65] W. Nickel, T. Weber, J.A. McNew, F. Parlati, T.H. Sollner, J.E. Rothman, Content mixing and membrane integrity during membrane fusion driven by pairing of isolated v-SNAREs and t-SNAREs, *Proc. Natl. Acad. Sci. U. S. A* 96 (1999) 12571–12576.
- [66] S.M. Dennison, M.E. Bowen, A.T. Brunger, B.R. Lentz, Neuronal SNAREs do not trigger fusion between synthetic membranes but do promote PEG-mediated membrane fusion, *Biophys. J.* 90 (2006) 1661–1675.
- [67] H. Yu, S.S. Rathore, J.A. Lopez, E.M. Davis, D.E. James, J.L. Martin, J. Shen, Comparative studies of Munc18c and Munc18-1 reveal conserved and divergent mechanisms of Sec1/Munc18 proteins, *Proc. Natl. Acad. Sci.* 110 (2013) E3271.
- [68] X. Liu, A.B. Seven, J. Xu, V. Esser, L. Su, C. Ma, J. Rizo, Simultaneous lipid and content mixing assays for *in vitro* reconstitution studies of synaptic vesicle fusion, *Nat. Protoc.* 12 (2017) 2014.
- [69] E. Karatekin, J.E. Rothman, Fusion of single proteoliposomes with planar, cushioned bilayers in microfluidic flow cells, *Nat. Protoc.* 7 (2012) 903–920.
- [70] T. Liu, W.C. Tucker, A. Bhalla, E.R. Chapman, J.C. Weisshaar, SNARE-driven, 25-millisecond vesicle fusion *in vitro*, *Biophys. J.* 89 (2005) 2458–2472.
- [71] M.E. Bowen, K. Wening, A.T. Brunger, S. Chu, Single molecule observation of liposome-bilayer fusion thermally induced by soluble N-ethyl maleimide sensitive-factor Attachment protein receptors (SNAREs), *Biophys. J.* 87 (2004) 3569–3584.
- [72] E.A. Smith, J.C. Weisshaar, Docking, not fusion, as the rate-limiting step in a SNARE-driven vesicle fusion assay, *Biophys. J.* 100 (2011) 2141–2150.
- [73] R.J. Rawle, B. van Lengerich, M. Chung, P.M. Bendix, S.G. Boxer, Vesicle fusion observed by content transfer across a tethered lipid bilayer, *Biophys. J.* 101 (2011) L37–L39.
- [74] K.M. Flavier, S.G. Boxer, Vesicle fusion mediated by solanesol-anchored DNA, *Biophys. J.* 113 (2017) 1260–1268.
- [75] D.L. Floyd, J.R. Ragains, J.J. Skehel, S.C. Harrison, A.M. van Oijen, Single-particle kinetics of influenza virus membrane fusion, *Proc. Natl. Acad. Sci.* 105 (2008) 15382.
- [76] D.A. Costello, D.W. Lee, J. Drewes, K.A. Vasquez, K. Kisler, U. Wiesner, L. Pollack, G.R. Whittaker, S. Daniel, Influenza virus-membrane fusion triggered by proton uncaging for single particle studies of fusion kinetics, *Anal. Chem.* 84 (2012) 8480–8489.
- [77] R.J. Rawle, S.G. Boxer, P.M. Kason, Disentangling viral membrane fusion from receptor binding using synthetic DNA-lipid conjugates, *Biophys. J.* 111 (2016) 123–131.
- [78] T. Ivanovic, J.L. Choi, S.P. Whelan, A.M. van Oijen, S.C. Harrison, Influenza-virus membrane fusion by cooperative fold-back of stochastically induced hemagglutinin intermediates, *eLife* 2 (2013) e00333.
- [79] J.J. Otterstrom, B. Brandenburg, M.H. Koldijk, J. Juraszek, C. Tang, S. Mashaghi, T. Kwaks, J. Goudsmit, R. Vogels, R.H.E. Friesen, A.M. van Oijen, Relating influenza virus membrane fusion kinetics to stoichiometry of neutralizing antibodies at the single-particle level, *Proc. Natl. Acad. Sci.* 111 (2014) E5143.
- [80] J.W. Kuhlmann, M. Junius, U. Diederichsen, C. Steinem, SNARE-mediated single-vesicle fusion events with supported and freestanding lipid membranes, *Biophys. J.* 112 (2017) 2348–2356.
- [81] R. Hubrich, Y. Park, I. Mey, R. Jahn, C. Steinem, SNARE-mediated fusion of single chromaffin granules with pore-spanning membranes, *Biophys. J.* 116 (2019) 308–318.
- [82] T.Y. Yoon, B. Okumus, F. Zhang, Y.K. Shin, T. Ha, Multiple intermediates in SNARE-induced membrane fusion, *Proc. Natl. Acad. Sci. U. S. A* 103 (2006) 19731–19736.

- [83] H.-K. Lee, Y. Yang, Z. Su, C. Hyeon, T.-S. Lee, H.-W. Lee, D.-H. Kweon, Y.-K. Shin, T.-Y. Yoon, Dynamic Ca^{2+} -dependent stimulation of vesicle fusion by membrane-anchored synaptotagmin 1, *Science* 328 (2010) 760.
- [84] T.-Y. Yoon, X. Lu, J. Diao, S.-M. Lee, T. Ha, Y.-K. Shin, Complexin and Ca^{2+} stimulate SNARE-mediated membrane fusion, *Nat. Struct. Mol. Biol.* 15 (2008) 707.
- [85] J. Diao, Z. Su, Y. Ishitsuka, B. Lu, K.S. Lee, Y. Lai, Y.-K. Shin, T. Ha, A single-vesicle content mixing assay for SNARE-mediated membrane fusion, *Nat. Commun.* 1 (2010) 54.
- [86] M. Kyoung, A. Srivastava, Y.X. Zhang, J.J. Diao, M. Vrljic, P. Grob, E. Nogales, S. Chu, A.T. Brunger, In vitro system capable of differentiating fast Ca^{2+} -triggered content mixing from lipid exchange for mechanistic studies of neurotransmitter release, *Proc. Natl. Acad. Sci. U. S. A* 108 (2011) E304–E313.
- [87] Y. Lai, J. Diao, Y. Liu, Y. Ishitsuka, Z. Su, K. Schulten, T. Ha, Y.-K. Shin, Fusion pore formation and expansion induced by Ca^{2+} and synaptotagmin 1, *Proc. Natl. Acad. Sci.* 2013, 110, 1333.
- [88] M. Winterhalter, Black lipid membranes, *Curr. Opin. Colloid Interface Sci.* 5 (2000) 250–255.
- [89] L. Chernomordik, A. Chanturiya, J. Green, J. Zimmerberg, The hemifusion intermediate and its conversion to complete fusion: regulation by membrane composition, *Biophys. J.* 69 (1995) 922–929.
- [90] A. Cypionka, A. Stein, J.M. Hernandez, H. Hippchen, R. Jahn, P.J. Walla, Discrimination between docking and fusion of liposomes reconstituted with neuronal SNARE-proteins using FCS, *Proc. Natl. Acad. Sci. U. S. A* 106 (2009) 18575–18580.
- [91] J.-Y. Kim, B.-K. Choi, M.-G. Choi, S.-A. Kim, Y. Lai, Y.-K. Shin, N.K. Lee, Solution single-vesicle assay reveals PIP(2)-mediated sequential actions of synaptotagmin-1 on SNAREs, *EMBO J.* 31 (2012) 2144–2155.
- [92] B.-K. Choi, M.-G. Choi, J.-Y. Kim, Y. Yang, Y. Lai, D.-H. Kweon, N.K. Lee, Y.-K. Shin, Large α -synuclein oligomers inhibit neuronal SNARE-mediated vesicle docking, *Proc. Natl. Acad. Sci.* 110 (2013) 4087.
- [93] N.C. Gauthier, T.A. Masters, M.P. Sheetz, Mechanical feedback between membrane tension and dynamics, *Trends Cell Biol.* 22 (2012) 527–535.
- [94] M. Herant, V. Heinrich, M. Dembo, Mechanics of neutrophil phagocytosis: behavior of the cortical tension, *J. Cell Sci.* 118 (2005) 1789.
- [95] M.I. Angelova, D.S. Dimitrov, Liposome electroformation, *Faraday Discuss* 81 (1986) 303–311.
- [96] M.I. Angelova, S. Soléau, P. Méléard, F. Faucon, P. Bothorel, Preparation of giant vesicles by external AC electric fields. Kinetics and applications, in: C. Helm, M. Lösche, H. Möhwald (Eds.), *Trends Coll. Interf. Sci.*, Steinkopff, 1992, pp. 127–131.
- [97] K.S. Horger, D.J. Estes, R. Capone, M. Mayer, Films of agarose enable rapid formation of giant liposomes in solutions of physiologic ionic strength, *J. Am. Chem. Soc.* 131 (2009) 1810–1819.
- [98] T. Tanaka, M. Yamazaki, Membrane fusion of giant unilamellar vesicles of neutral phospholipid membranes induced by La^{3+} , *Langmuir* 20 (2004) 5160–5164.
- [99] D.V. Volodkin, V. Ball, J.-C. Voegel, H. Möhwald, R. Dimova, V. Marchi-Artzner, Control of the interaction between membranes or vesicles: adhesion, fusion and release of dyes, *Colloids Surf. Physicochem. Eng. Aspects* 303 (2007) 89–96.
- [100] J. Heuvingh, F. Pincet, S. Cribier, Hemifusion and fusion of giant vesicles induced by reduction of inter-membrane distance, *Europ. Phys. J. E* 14 (2004) 269–276.

- [101] C.K. Haluska, K.A. Riske, V. Marchi-Artzner, J.M. Lehn, R. Lipowsky, R. Dimova, Time scales of membrane fusion revealed by direct imaging of vesicle fusion with high temporal resolution, *Proc. Natl. Acad. Sci. U. S. A* 103 (2006) 15841–15846.
- [102] N. Kahya, E.I. Pecheur, W.P. de Boeij, D.A. Wiersma, D. Hoekstra, Reconstitution of membrane proteins into giant unilamellar vesicles via peptide-induced fusion, *Biophys. J.* 81 (2001) 1464–1474.
- [103] D. Tareste, J. Shen, T.J. Melia, J.E. Rothman, SNAREpin/Munc18 promotes adhesion and fusion of large vesicles to giant membranes, *Proc. Natl. Acad. Sci. U. S. A* 105 (2008) 2380–2385.
- [104] D.P. Pantazatos, R.C. MacDonald, Directly observed membrane fusion between oppositely charged phospholipid bilayers, *J. Membr. Biol.* 170 (1999) 27–38.
- [105] G.H. Lei, R.C. MacDonald, Lipid bilayer vesicle fusion: intermediates captured by high-speed microfluorescence spectroscopy, *Biophys. J.* 85 (2003) 1585–1599.
- [106] K.A. Riske, N. Bezlyepkina, R. Lipowsky, R. Dimova, Electrofusion of model lipid membranes viewed with high temporal resolution, *Biophys. Rev. Lett.* 4 (2006) 387–400.
- [107] A. Rørvig-Lund, A. Bahadori, S. Semsey, P.M. Bendix, L.B. Oddershede, Vesicle fusion triggered by optically heated gold nanoparticles, *Nano Lett.* 15 (2015) 4183–4188.
- [108] A. Bahadori, L.B. Oddershede, P.M. Bendix, Hot-nanoparticle-mediated fusion of selected cells, *Nano Res.* 10 (2017) 2034–2045.
- [109] A. Bahadori, G. Moreno-Pescador, L.B. Oddershede, P.M. Bendix, Remotely controlled fusion of selected vesicles and living cells: a key issue review, *Rep. Prog. Phys.* 81 (2018) 032602.
- [110] R. Shirakashi, V.L. Sukhorukov, R. Reuss, A. Schulz, U. Zimmermann, Effects of a pulse electric field on electrofusion of giant unilamellar vesicle (GUV)-Jurkat cell (measurement of fusion ratio and electric field analysis of pulsed GUV-jurkat cell), *J. Therm. Sci. Tech. Jpn.* 7 (2012) 589–602.
- [111] T. Robinson, P.E. Verboket, K. Eyer, P.S. Dittrich, Controllable electrofusion of lipid vesicles: initiation and analysis of reactions within biomimetic containers, *Lab Chip* 14 (2014) 2852–2859.
- [112] A. Strömberg, F. Ryttsén, D.T. Chiu, M. Davidson, P.S. Eriksson, C.F. Wilson, O. Orwar, R.N. Zare, Manipulating the genetic identity and biochemical surface properties of individual cells with electric-field-induced fusion, *Proc. Natl. Acad. Sci.* 97 (2000) 7.
- [113] N. Bezlyepkina, R.S. Gracià, P. Shchelokovskyy, R. Lipowsky, R. Dimova, Phase diagram and tie-line determination for the ternary mixture DOPC/eSM/Cholesterol, *Biophys. J.* 104 (2013) 1456–1464.
- [114] Y. Sun, C.-C. Lee, H.W. Huang, Adhesion and merging of lipid bilayers: a method for measuring the free energy of adhesion and hemifusion, *Biophys. J.* 100 (2011) 987–995.
- [115] P. Yang, R. Dimova, Nanoparticle synthesis in vesicle microreactors, in: A. George (Ed.), *Biomimetic Based Applications*, InTech, 2011, pp. 523–552.
- [116] P. Yang, R. Lipowsky, R. Dimova, Nanoparticle formation in giant vesicles: synthesis in biomimetic compartments, *Small* 5 (2009) 2033–2037.
- [117] A.C. Saito, T. Ogura, K. Fujiwara, S. Murata, S.M. Nomura, Introducing micrometer-sized artificial objects into live cells: a method for cell-giant unilamellar vesicle electrofusion, *PLoS One* 9 (2014).
- [118] H. Maruyama, N. Inoue, T. Masuda, F. Arai, Selective injection and laser manipulation of nanotool inside a specific cell using Optical pH regulation and optical tweezers, 2011 IEEE International Conference on Robotics and Automation, 2011, pp. 2674–2679.

- [119] A. Witkowska, R. Jahn, Rapid SNARE-mediated fusion of liposomes and chromaffin granules with giant unilamellar vesicles, *Biophys. J.* 113 (2017) 1251–1259.
- [120] S.-T. Yang, V. Kiessling, J.A. Simmons, J.M. White, L.K. Tamm, HIV gp41-mediated membrane fusion occurs at edges of cholesterol-rich lipid domains, *Nat. Chem. Biol.* 11 (2015) 424.
- [121] S.-T. Yang, A.J.B. Kreutzberger, V. Kiessling, B.K. Ganser-Pornillos, J.M. White, L.K. Tamm, HIV virions sense plasma membrane heterogeneity for cell entry, *Sci. Adv.* 3 (2017) e1700338.
- [122] S.-T. Yang, V. Kiessling, L.K. Tamm, Line tension at lipid phase boundaries as driving force for HIV fusion peptide-mediated fusion, *Nat. Commun.* 7 (2016) 11401.
- [123] P. Chlanda, E. Mekhedov, H. Waters, C.L. Schwartz, E.R. Fischer, R.J. Ryham, F.S. Cohen, P.S. Blank, J. Zimmerberg, The hemifusion structure induced by influenza virus haemagglutinin is determined by physical properties of the target membranes, *Nat. Microbiol.* 1 (2016) 16050.
- [124] S. Haldar, E. Mekhedov, C.D. McCormick, P.S. Blank, J. Zimmerberg, Lipid-dependence of target membrane stability during influenza viral fusion, *J. Cell Sci.* 132 (2019) jcs218321.
- [125] S. Trier, J.R. Henriksen, T.L. Andresen, Membrane fusion of pH-sensitive liposomes – a quantitative study using giant unilamellar vesicles, *Soft Matter* 7 (2011) 9027–9034.
- [126] O. Biner, T. Schick, Y. Muller, C. von Ballmoos, Delivery of membrane proteins into small and giant unilamellar vesicles by charge-mediated fusion, *FEBS Lett.* 590 (2016) 2051–2062.
- [127] N. Kahya, D.A. Wiersma, B. Poolman, D. Hoekstra, Spatial organization of bacteriorhodopsin in model membranes: light-induced mobility changes, *J. Biol. Chem.* 277 (2002) 39304–39311.
- [128] R.B. Lira, T. Robinson, R. Dimova, K.A. Riske, Highly efficient protein-free membrane fusion: a giant vesicle study, *Biophys. J.* 116 (2019) 79–91.
- [129] A. Csiszar, N. Hersch, S. Dieluweit, R. Biehl, R. Merkel, B. Hoffmann, Novel fusogenic liposomes for fluorescent cell labeling and membrane modification, *Bioconjug. Chem.* 21 (2010) 537–543.
- [130] R.B. Lira, M.A.B.L. Seabra, A.L.L. Matos, J.V. Vasconcelos, D.P. Bezerra, E. de Paula, B.S. Santos, A. Fontes, Studies on intracellular delivery of carboxyl-coated CdTe quantum dots mediated by fusogenic liposomes, *J. Mater. Chem. B* 1 (2013) 4297–4305.
- [131] V.N. Georgiev, A. Grafmüller, D. Bléger, S. Hecht, S. Kunstmann, S. Barbirz, R. Lipowsky, R. Dimova, Area increase and budding in giant vesicles triggered by light: behind the scene, *Adv. Sci.* 5 (2018) 1800432.
- [132] B. Mattei, A.D.C. Franca, K.A. Riske, Solubilization of binary lipid mixtures by the detergent triton X-100: the role of cholesterol, *Langmuir* 31 (2015) 378–386.
- [133] P. Gipson, Y. Fukuda, R. Danev, Y. Lai, D.-H. Chen, W. Baumeister, A.T. Brunger, Morphologies of synaptic protein membrane fusion interfaces, *Proc. Natl. Acad. Sci.* 114 (2017) 9110.
- [134] J. Otterstrom, A.M. van Oijen, Visualization of membrane fusion, one particle at a time, *Biochemistry* 52 (2013) 1654–1668.